AD-A179 206

UNSTEADY HEAT TRANSFER RESULTING FROM
THE RAPID CHARGING OF AN EVACUATED
TANK WITH CONDUCTING WALLS

THESIS

Dennis E. Lilelkis
Second Lieutenant, USAF

AFIT/GA/AA/86D-9

DEPARTMENT OF THE AIR FORCE

AIR UNIVERSITY

AIR FORCE INSTITUTE OF TECHNOLOGY
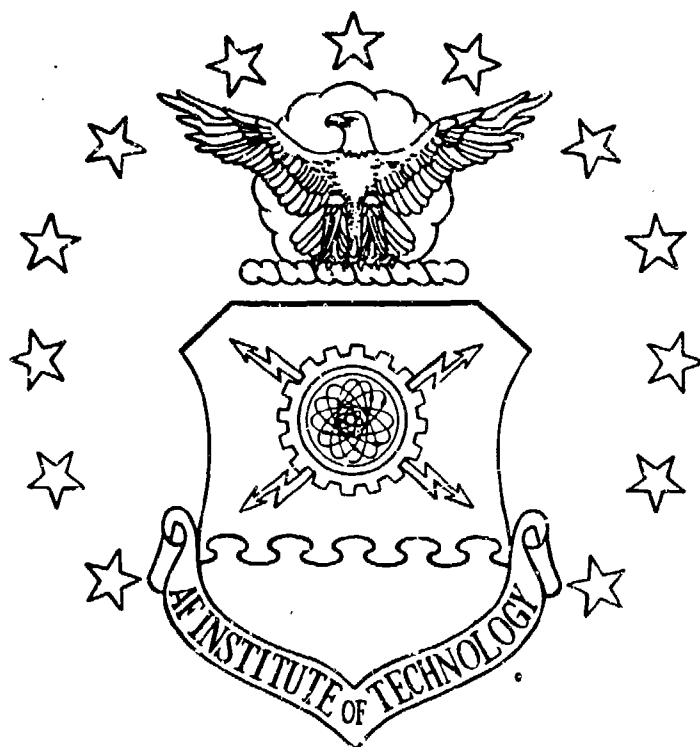
Wright-Patterson Air Force Base, Ohio

87 4   16 01t

DTIC
ELECTED
S
APR 1 7 1987
D
D

UNSTEADY HEAT TRANSFER RESULTING FROM
THE RAPID CHARGING OF AN EVACUATED
TANK WITH CONDUCTING WALLS

THESIS

Dennis E. Lileikis
Second Lieutenant, USAF

AFIT/GA/AA/86D-9

AFIT/GA/AA/86D-9

UNSTEADY HEAT TRANSFER RESULTING FROM THE RAPID

CHARGING CF AN EVACUATED TANK WITH CONDUCTING WALLS

THESIS

Presented to the Faculty of the School of Engineering

of the Air Force Institute of Technology

Air University

In Partial Fulfillment of the

Requirements for the Degree of

Master of Science in Astronautical Engineering

Dennis E. Lilelkis, B.S.

Second Lieutenant, USAF

December 1986

Preface

> The time will come when
> diligent research over long periods
> will bring to light things which now
> lie hidden. A single lifetime ...
> would not be enough for the investi-
> gation of so vast a subject ... Many
> discoveries are reserved for ages yet
> to come ...
>
> Seneca, Natural Questions
> Book 7, first century

As is so often the case in scientific research, the experimenter, in his desire to uncover the truth, unearths more questions than he answers. I can now empathize with that scientist after having worked for so long on this thesis. As data was slowly acquired, so too were theories to explain the results. However, further data reduction would often prove the hypothesis in error, and a re-thinking was in order. Yet when data and theory finally agree, you enjoy a wonderful sense of accomplishment. As Democritus of Abdera once said, "I would rather understand one cause than be King of Persia."

None of this, however, would have been possible without the help of several individuals. First and foremost is Dr. James Hitchcock, my thesis advisor. I first became interested in heat transfer during an introductory course which he had taught. Throughout my entire heat transfer curriculum, I have always been eager to learn from and study under Dr. Hitchcock. Secondly, I would like to thank 2Lt.

James Shoemaker, a member of the AFWAL Propulsion Lab, for
the use of his digitization equipment. Thanks also go out to
Mr. John Brohas and the AFIT lab technicians for their help
in constructing my apparatus.

.

Computer used for word processing ...... Apple IIc

Program used .... Appleworks

Printer used .... Imagewriter II

Table of Contents

List of Figures

List of Symbols

	Quantity	Units
A	Area	ft^2
α	Thermal Diffusivity	ft^2/s
c_p	Specific Heat at Constant Pressure	lbf-ft/lbm-R
c_v	Specific Heat at Constant Volume	lbf-ft/lbm-R
e	Stored Energy per Unit Mass	BTU/lbm
E	Voltage or Stored Energy	Volts or BTU
G	Amplifier Gain	---
γ	Ratio of Specific Heats c_p/c_v	---
g_c	Conversion Constant	32.2 lbm-ft/lbf-s^2
h	Convection Coefficient	BTU/ft^2-s-F
i	Total Enthalpy per Unit Mass	BTU/lbm
I	Current	Amps
m	Mass	lbm
M	Mach Number	---
P	Pressure	lbf/ft^2
q	Heat Flux	BTU/ft^2-s
Q	Heat	BTU
R	Resistance or Gas Constant	Ohms or lbf-ft/lbm-R
ρ	Density	lbm/ft^3
s	Entropy per Unit Mass	BTU/lbm
S	Entropy	BTU
t	Time	s
T	Temperature	F or R

| u | Velocity | ft/s |
| V | Volume | ft^3 |

Subscripts

c.v.	Control Volume
f	Final condition
g	Gage property
i	Initial condition or index of summation
N	A given time increment in a summation
o	Ambient or atmospheric condition
p	Pressure in tank equal to atmospheric pressure
s	Surface condition
t	Derivative with respect to time
th	Nozzle throat condition
uc	Unchoked condition
x	Derivative with respect to x

Overstrike

| • | Derivative with respect to time |

Abstract

The two classical problems of charging a tank with an
ideal gas concern themselves only with the initial and final
states of the gas. The first problem involves an insulated
tank. From initial conditions, the final temperature of the
gas in the tank can be determined. The second problem
involves a tank with conducting walls. In this case, it is
the total heat transferred from the gas to the tank walls
which can be found. This study went beyond these equilibrium
analyses to acquire a fundamental understanding of the
transient phenomenon involved in charging a tank.

By way of experimentation, transient pressure and heat
flux measurements were made on an evacuated cylindrical tank
as it was charged by sudden exposure to the atmosphere.
Then, an average convection coefficient and driving
temperature potential for the tank were found. A method was
then developed for estimating heating rates for other tanks
and different ambient conditions. Also, information about
the transient flow dynamics occurring within the tank was
gleaned from the heat transfer data. This information
includes rates of kinetic, internal, and thermal energy
generation and dissipation as well as rates of entropy
creation in the gas.

UNSTEADY HEAT TRANSFER RESULTING FROM THE RAPID
CHARGING OF AN EVACUATED TANK WITH CONDUCTING WALLS

I. Introduction

The classical problem of charging a tank with an ideal
gas is well documented for two conditions [1:80-87]
[2:203-210]. If an insulated tank is considered, the final
equilibrium temperature can be determined. If, on the other
hand, the tank has a conducting wall, the total heat
transferred from the gas to the wall can be determined. In
either case, the solution is derived from an elementary
application of the first law of thermodynamics. The change
in stored energy in the tank must equal the difference
between the energy which came into the tank, be it internal,
kinetic, or flow energy, and the heat lost from the fluid to
the tank walls.

In contrast, little if any work has been done to
understand the actual transient process involved in charging
a vessel. Thorough literature searches, both manual and
computer, revealed no useful information regarding this
process. Perhaps one reason for the lack of information is
that no analytical solution exists for the unsteady process
of charging a tank with a fluid. Because of the complexity
of the flow, an analytical solution would require that the

1

Navier-Stokes equations be solved in their entirety.
Significant simplifications cannot be made to these equations
since both compressibility and diffusive transport of
momentum and energy dominate the entire process. The
diffusive processes are what dictate the rate of kinetic
energy dissipation in the tank as well as the rate of heat
transfer to the walls. As a consequence, a simple energy
balance will not work. The only alternative, then, is an
experimental investigation. With the rapid-response,
thin-film resistance gages currently available, the rate of
heat transfer encountered during the charging of a tank may
be observed directly, thereby yielding some insight into the
dynamics of the flow.

There were three main objectives of the study. The
first objective was to detail the distribution of the
measured thermal energy along the walls of the tank by direct
observation. The second objective was to use the measured
heat flux data to derive an average convection coefficient
and its associated temperature difference. These could then
be used to predict heat flux rates encountered during the
charging of other tanks. Finally, the third objective was to
gain some knowledge of the flow dynamics that occur within a
tank during the charging process.

II. Charging Theory

Charging is the process by which a vessel containing a fluid at low pressure is filled from a reservoir of fluid at a high pressure. The resulting pressure gradient forces fluid from the reservoir into the vessel until the pressures inside and out are equal. The work done in moving this mass of fluid is then manifested in the internal and kinetic energies of the fluid in the vessel as well as any heat lost to the surroundings.

For example, assume that a perfectly evacuated, insulated tank is suddenly opened to atmospheric pressure. This is one of the two classical problems that has been solved. The mass which enters the tank carries with it internal energy as well as flow work done by the atmosphere in pushing the mass into the tank. This total enthalpy per unit mass is just $c_p T_0$. After the air comes to rest in the tank, it has energy per unit mass of $c_v T_f$. See Figure 2-1. Since the tank is perfectly insulated, no energy is lost to the walls by way of heat transfer. Thus, a simple energy balance can be written to find the final temperature of the air in the tank. Enthalpy in, $mc_p T_0$, must equal energy stored in the tank, $mc_v T_f$. The final temperature of the gas, therefore, equals $T_0 c_p / c_v$. For air, if $T_0 = 530$ R, the final temperature would be 742 R, an increase of 212 R.
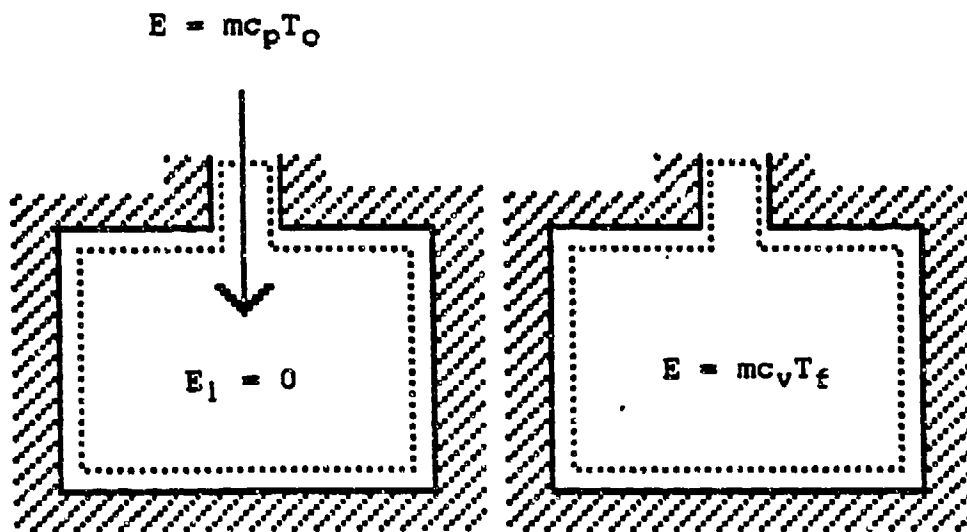
Figure 2-1   The Charging of an Evacuated, Insulated Tank
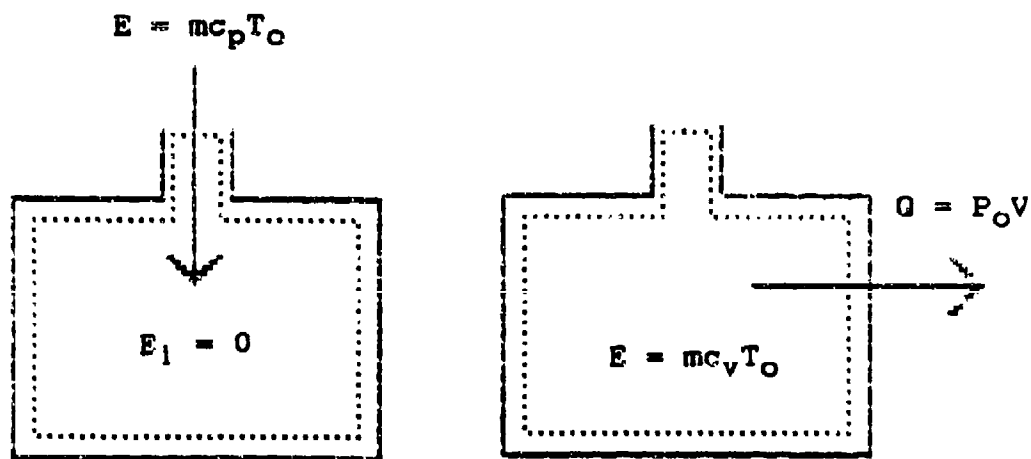
Figure 2-2   The Charging of an Evacuated Tank with
Conducting Walls

4

In the second classical problem, the tank walls are conductors of heat, and the total heat transferred to these walls is sought. Once again, assume an evacuated tank that is opened suddenly to the atmosphere. After the air in the tank comes to equilibrium, it will have the same pressure and temperature as it had before entering the tank. See Figure 2-2. All the flow work done by the atmosphere will be manifested in the heat transfer to the tank walls. This flow work per unit mass is P_o/ρ_o. Therefore $Q = mP_o/\rho_c = P_oV$ where P_o is the atmospheric pressure and V is the volume of the tank.

During the transient charging period, the actual rise in fluid temperature within the uninsulated tank is a complex function of the rate of kinetic energy dissipation in the tank as well as the rate of heat dissipation to the tank walls. To determine the heat that is lost as a function of time, the first law of thermodynamics in its open, unsteady form is needed. This law states that the increase in stored energy within the tank must equal the enthalpy added by the mass which enters the tank minus the heat that is removed from the gas at each instant in time. Consider the control volume pictured in Figure 2-3. Mathematically,

$$\int dE = \int \dot{m} \, i \, dt - \iint q \, dA \, dt \qquad [2-1]$$

Also,

$$dE = d(mc_vT + mu^2/2g_c) \qquad [2-2]$$

5
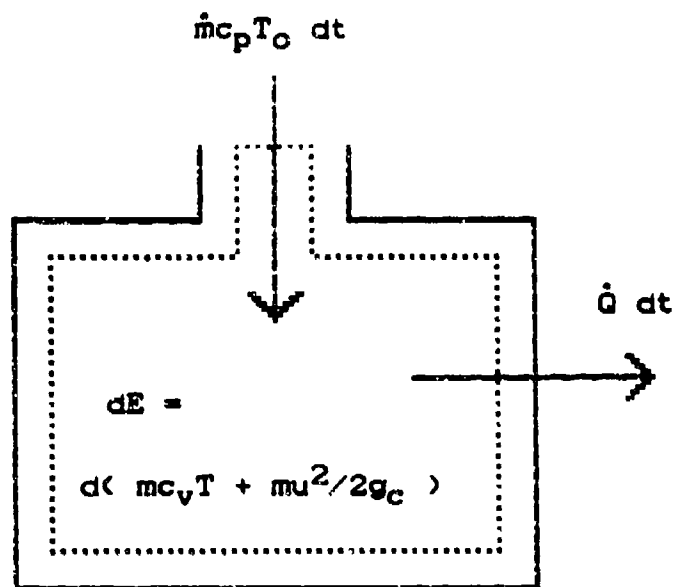
Figure 2-3   Control Volume Used in the Transient Energy
Balance of Equation [2-3]
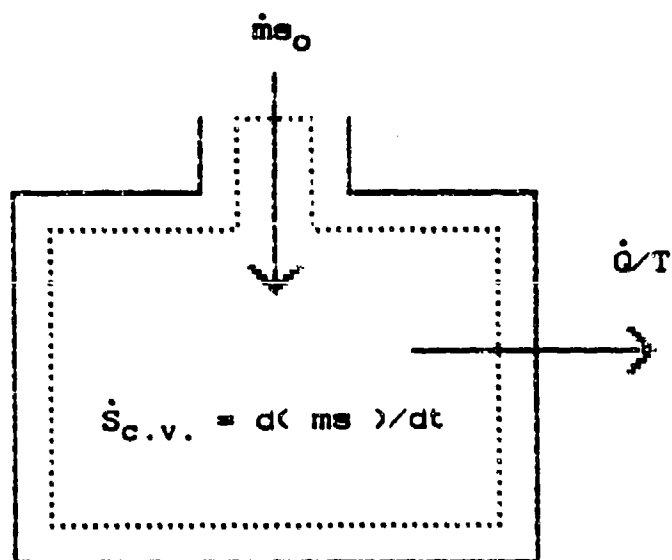
Figure 2-4   Control Volume Used in the Transient Entropy
Balance of Equation [2-4]

6

T and u represent some average temperature and velocity of the mass within the tank.

Equation [2-2] can be substituted into Eq. [2-1] and, assuming constant enthalpy entering the tank, the resulting integrals evaluated, yielding

$$m[c_vT + v^2/2g_c] - m_ic_vT_o = (m-m_i)c_pT_o - Q \qquad [2-3]$$

The term $m_ic_vT_o$ accounts for the initial mass in the tank if it was not fully evacuated. Q is the total heat that has been transferred from the gas to the tank walls.

A second law analysis of this transient problem can also be accomplished. The second law of thermodynamics states that the rate at which entropy is created within the control volume must be greater than or equal to the rate at which entropy enters with the entering mass minus the rate at which entropy leaves by way of heat transfer. See Figure 2-4. This can be expressed as

$$\dot{S}_{c.v.} \geq \dot{m}s_o - \dot{Q}/T \qquad [2-4]$$

$\dot{S}_{c.v.}$ is the rate of entropy increase within the tank, s_o is the specific entropy of the fluid entering the tank, and $\dot{Q}/T$ is the rate at which entropy leaves the gas due to heat transfer. T is the temperature of the inner tank wall which, for walls having large heat capacity and conductivity, equals T_o. The entropy per unit mass of the air within the tank can be found by

7

$$s(t) = s_o + c_p \ln[T(t)/T_o] - R \ln[P(t)/P_o] \qquad [2-5]$$

Thus, data derived from Eq. [2-5] can be numerically differentiated to find $\dot{S}_{c.v.}(t)$ providing, of course, that the mass within the tank is known since

$$\dot{S}_{c.v.}(t) = d(m(t) s(t))/dt \qquad [2-6]$$

III. Thin-film Gage Theory

Surface Temperatures

Thin-film resistance gages were used to measure the temperature at the surface of a solid substrate. On the surface of the substrate is a thin strip of platinum through which a small, constant current is passed. The resistance change of the platinum film is directly proportional to its change in temperature above some reference temperature. The resistance of the film at a given temperature is

$$R_g(T) = R_g(T_{ref}) + (T-T_{ref}) (\Delta R / \Delta T)_g \qquad [3-1]$$

$(\Delta R / \Delta T)_g$ is a property of an individual gage determined from calibration. [3:5]

The resistance change of the film can be measured by measuring the voltage change across it. A gage can be connected to a bridge and amplifier circuit as shown in Figure 3. The bridge element resistor that is shown in series with the gage should be large enough to ensure that the change in gage resistance does not induce an appreciable change in current. For this type of constant-current bridge circuit, the resistance change is given by the measured voltage change.

$$\Delta R_g = \Delta E (R+R_g)/RI_g G \qquad [3-2]$$

10 Volts

1000Ω

1000Ω

0 ~ 1000Ω

Rg

Amplifier Gain

G
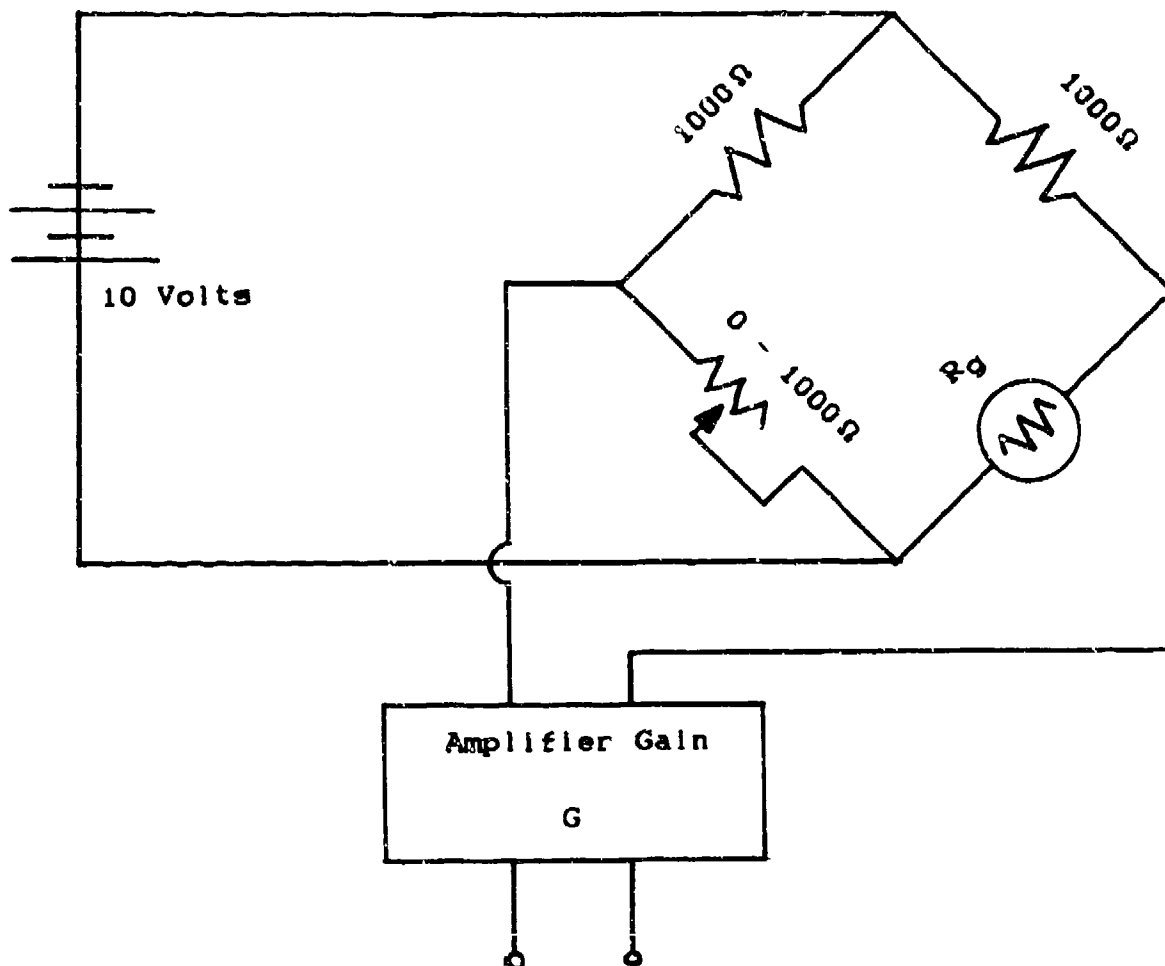
Figure 3   Bridge Circiut Used with the Thin-film Gages

10

E is the measured voltage across the bridge, I_g is the constant current through the gage, and G is the gain of the amplifier. [3]

By using Eq. [3-1] and [3-2], the change in voltage can be directly converted to change in temperature with the following expression.

$$\Delta T = \Delta E \ (\ R+R_g(T_{ref})+R'[T - T_{ref}] \ )^2 \ / \ RVGR' \qquad [3-3]$$

where $R' = (\Delta R/\Delta T)_g$. Note that current has been eliminated in favor of the applied voltage, V.

Surface Heat Fluxes

Although thin-film gages measure temperature, heat flux can be determined by using a solution to the basic heat equation with two assumptions imposed. First, the gage is treated as a semi-infinite solid during the test time. Second, the heat flux through the gage is assumed to propagate in a one-dimensional fashion. These elements allow heat flux rates to be determined from the temperature data.

To solve for the surface heat flux in terms of surface temperature, the one-dimensional heat equation can be used

$$T^+_t = \alpha \ T^+_{xx} \qquad [3-4]$$

where $T^+ = T^+(x,t) = T(x,t) - T(x,0)$.

The boundary conditions are

11

$$T^+(0,t) = T^+_s$$
$$T^+(x \to \infty, t) \to 0$$
$$T^+(x,0) = 0$$

The solution to this equation can be found by using a similarity variable or by the the Laplace transform technique. [4:384-390]

$$T^+ = T^+_s \, \text{erfc}(\, x \, / \, [2(\alpha t)^{1/2}] \,) \qquad [3\text{-}5]$$

An energy balance at the surface of the gage requires that the heat flux incident on the gage must equal the heat flux into the gage. Mathematically,

$$q(t) = - k \, T^+_x \, |_{x=0} \qquad [3\text{-}6]$$

Cook and Felderman [5] used Eq. [3-5] and [3-6] along with Duhammel's superposition method [4:403-411] to obtain a numerical solution for surface heat flux given a discrete number of measured surface temperatures. Their equation, slightly rearranged, is

$$q(t_N) = 2\sqrt{\frac{\rho c k}{\pi}} \left[\frac{T^+_s(t_0)}{2t_N^{1/2}} + \sum_{l=1}^{N} \frac{T^+_s(t_l) - T^+_s(t_{l-1})}{(t_N - t_l)^{1/2} + (t_N - t_{l-1})^{1/2}} \right] \quad [3\text{-}7]$$

Thus, given the measured temperatures from a thin-film resistance gage, surface heat fluxes may be calculated as a function of time.

IV. The Experiment

Apparatus

The Tank. The tank was fabricated from a section of
stainless steel pipe 0.375 inch thick. The tank had an inner
diameter of 10 inches and a length of 35 13/16 inches. Holes
were bored and tapped at various locations on the tank to
accommodate instrumented brass plugs. See Figure 4-1. The
top and bottom plates were made from steel and provided with
sites for instrumented plugs as well. The bottom plate was
welded in place, while the top one was bolted to the tank.
This provided a means of entering the tank should the need
arise. All touching metal parts that were not welded
together had O-ring seals or rubber gaskets between them to
prevent leakage.

The entrance to the tank consisted of a simple
converging nozzle. The nozzle had an entrance diameter of 4
inches and a throat diameter of 1 inch, yielding an area
ratio of 16. A rubber stopper commonly found in chemistry
labs was used to plug the nozzle during evacuation. The
stopper was attatched to one arm of a lever which was bolted
to the top of the tank. This lever was used to initiate the
flow quickly by pulling the stopper out and away from the
nozzle inlet.

Thin-film Gages. Five thin-film gages were used to
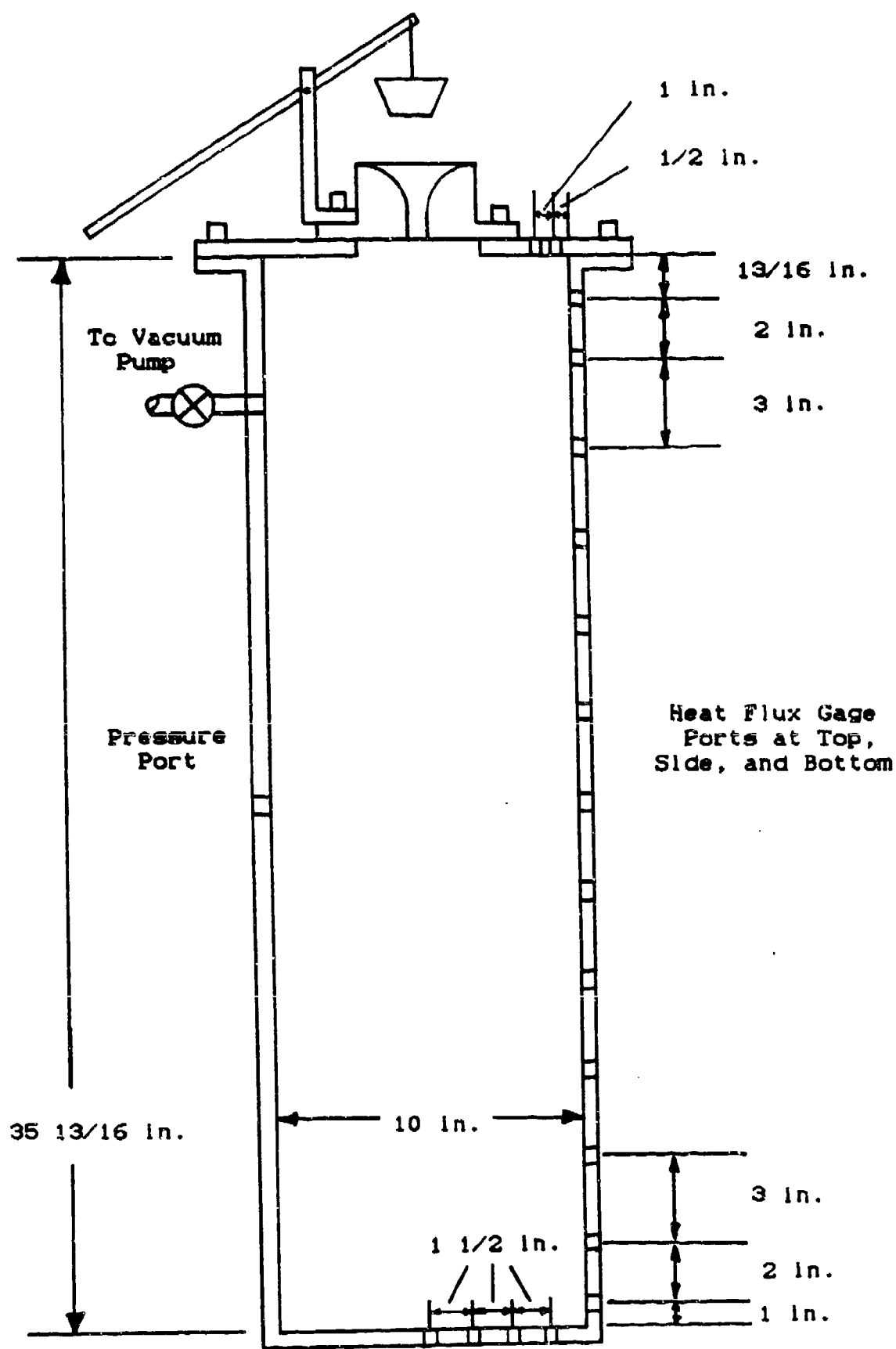gather data on the rates of heat transfer at 19 different

13

Figure 4-1   Tank Apparatus Used In Charging Experiments

stations over the tank. The gages were commercially produced and consisted of a thin strip of platinum which was deposited onto one end of a cylindrical piece of quartz. The quartz substrate was 0.25 inch long and had a diameter of 0.125 inch. Each gage was inserted into a hollow plexiglas rod which had an outer diameter of 0.3875 inch. This rod was then affixed inside a hollow brass plug. See Figure 4-2. Epoxy was used to hold the plexiglas and quartz in place as well as to ensure an airtight seal. When inserted into the tank, the center of each gage was flush with the inner wall of the tank; the edges were slightly recessed due to the curvature of the tank wall.

The gages were connected to bridge/amplifier circuits. The output from each bridge was stored using a digital waveform recorder. After a run, each of the five recorded channels was displayed on an oscilliscope, and a polaroid photograph was taken of the resulting trace. The photo was later digitized and the data stored in a computer for data reduction.

Pressure Transducer. An Endevco 0-100 psia pressure transducer was used to measure the transient pressure within the tank. The transducer and its signal conditioner fed data to the same digital waveform recorder. A polaroid photograph was taken and digitized and the data was stored in a computer for later reduction. A mercury manometer was used to
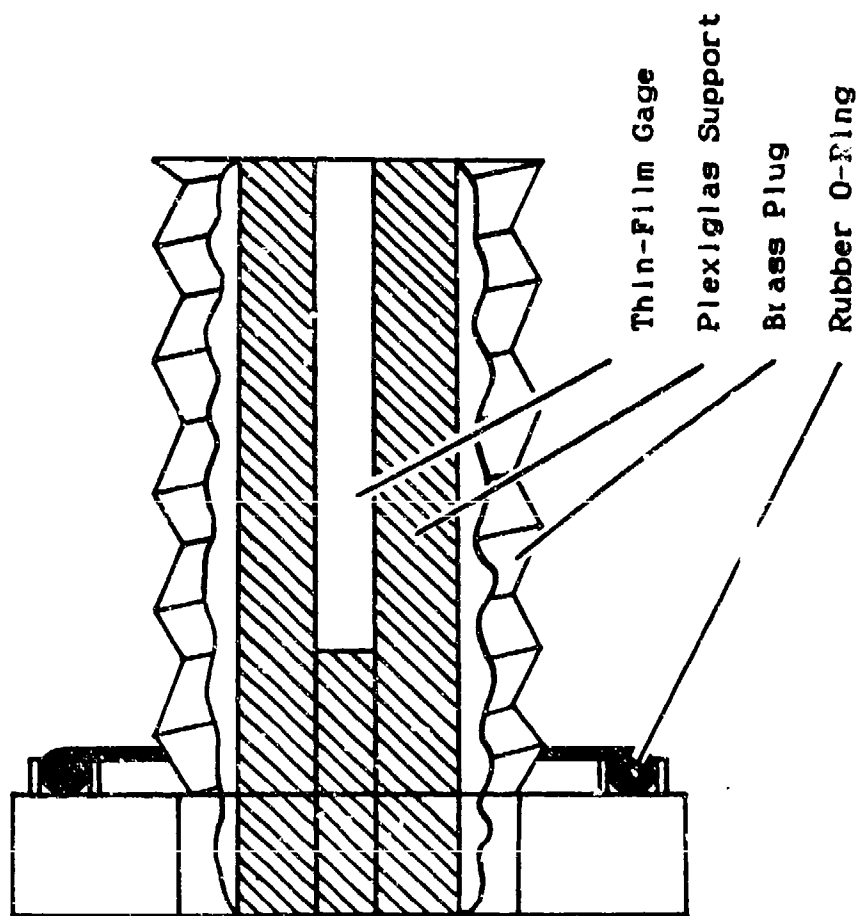
Figure 4-2   Thin-Film Gage in Brass Mounting Plug

Thin-Film Gage

Plexiglas Support

Brass Plug

Rubber O-Ring

16

calibrate the transducer while a mercury barometer was used
to determine atmospheric pressure.

Vacuum Pump. A mechanical vacuum pump was used to
evacuate the tank. The pump was connected to a valve which
was attached to the side of the tank. It was consistently
able to reduced the tank pressure to between 2 and 3 psia
within 5 to 7 minutes.

Digital Waveform Recorder. A Datalab 8 channel digital
waveform recorder was used to capture the data from the
thin-film and pressure gages. It was desired to use the
digitized data directly, but a suitable computer was
unavailable. Thus, the information stored in the recorder
was displayed on an oscilliscope, photographed, and then
digitized using other equipment.

Digitizer/Computer. A Hewlet-Packard plotter/ digitizer
was used to digitize the thin-film and pressure traces. This
data was then input by hand into an Apple IIc computer for
reduction and manipulation.

Pressure Gage Calibration

To calibrate the pressure transducer, the tank was
evacuated eight different times to various pressure levels.
Each time, the pressure from a mercury manometer was recorded
along with the deflection of the transducer trace on the
ocsilliscope. These measurements gave conversion constants
(from millivolts to psi) which varied by not more than 4%.

17

These eight constants were then averaged together to give a conversion constant of 2.88 mV/psi.

Next, to determine which location on the tank would give the "best" average pressure, the transient pressure was recorded at the top, the middle, and the bottom of the tank. There was no perceptible difference in the three traces. As a result, the pressure was assumed to be essentially constant throughout the entire tank at each instant in time. Since the location of the transducer was unimportant, the middle location was chosen for all subsequent runs as a matter of convenience.

Heat Flux Gage Calibration

Due to the difficulty in calibrating these types of gages [3], the calibration from the manufacturer was assumed to be correct. Each of the gages had different resistances and different rates of resistance change with temperature change. Care was taken during all test runs to keep track of each gage and the position on the tank which it occupied at that time.

Because thin-film gages work on a one-dimensional heat flow model (see Section III), the long times of this experiment (i.e. > 1 second) caused some concern as to whether two-dimensional effects might alter the results. In order to find out, one of the gages was exposed to a constant heat flux and the resulting signal recorded. Since an

analytic solution exists for this boundary condition, the response of the gage could be compared to a true one-dimensional model. The source of the constant heat flux was the stagnation region of a hot stream of air. This stream was generated with a hot air gun which is normally used to shrink electrical insulation. In actuality, it is the Nusselt number or convection coefficient which remains constant in stagnation region heat transfer. However, if the surface temperature of the gage is assumed to remain essentially constant, then heat flux will also be constant.

The test was crude and the hot stream only somewhat constant, but the results indicated that the gage was giving approximately one-dimensional results all the way out to 7 seconds. According to the analytic solution, a constant heat flux would result in an increase in surface temperature proportional to the square root of time. This would generate a horizontal line as plotted in Figure 4-3. Between 0 and 1 second for the low heat flux levels, there were small deviations from a horizontal line. This was due to the transient effects associated with establishing the stream of air onto the gage. The difference was much greater for the two highest heat flux levels where it was necessary to have the fan on the gun set on high. Apparently, this increased the transient flow establishment time. After the transient time period, however, the curves do approximate a straight, horizontal line. However, the curves generated with the two
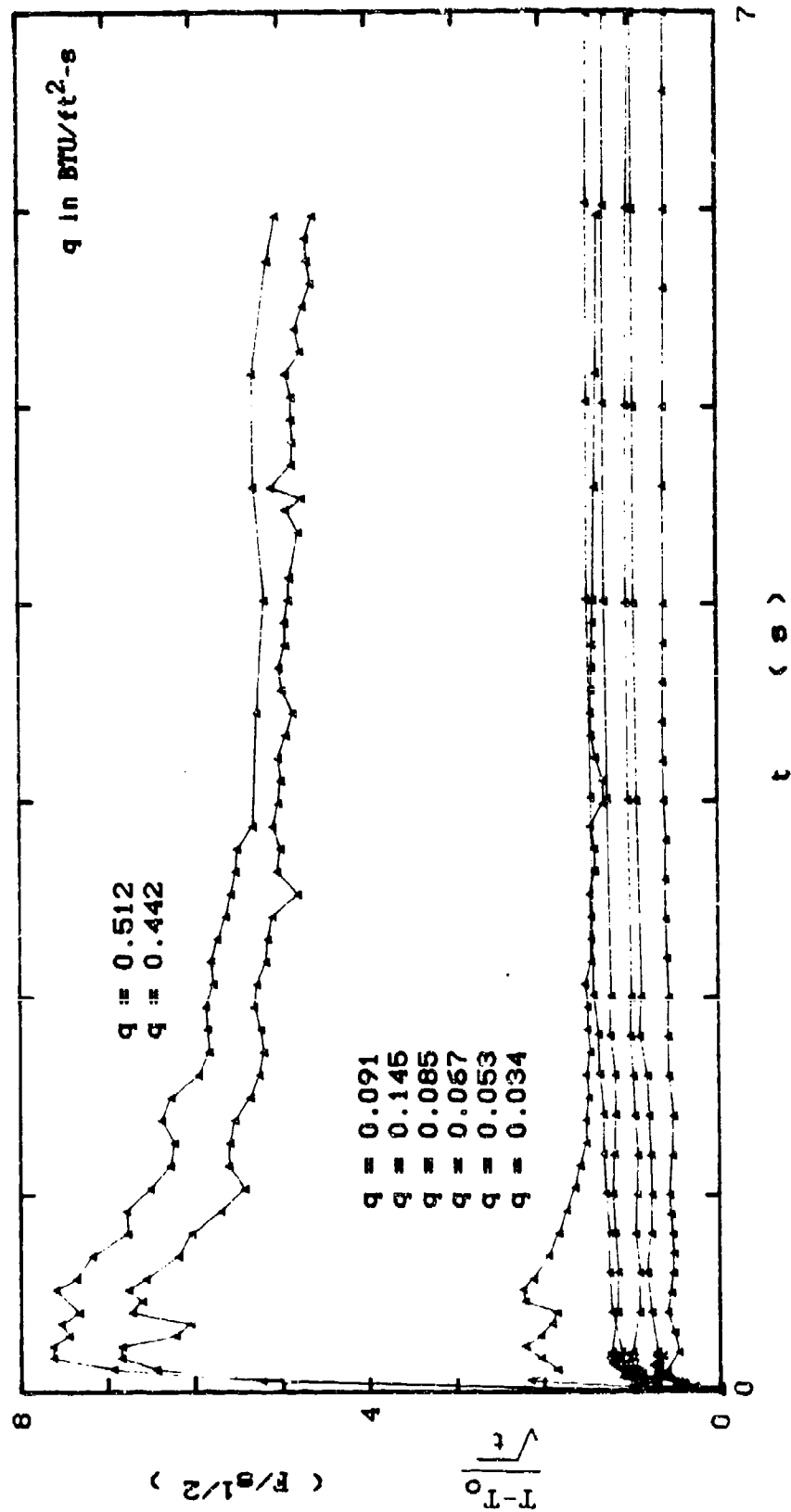
19

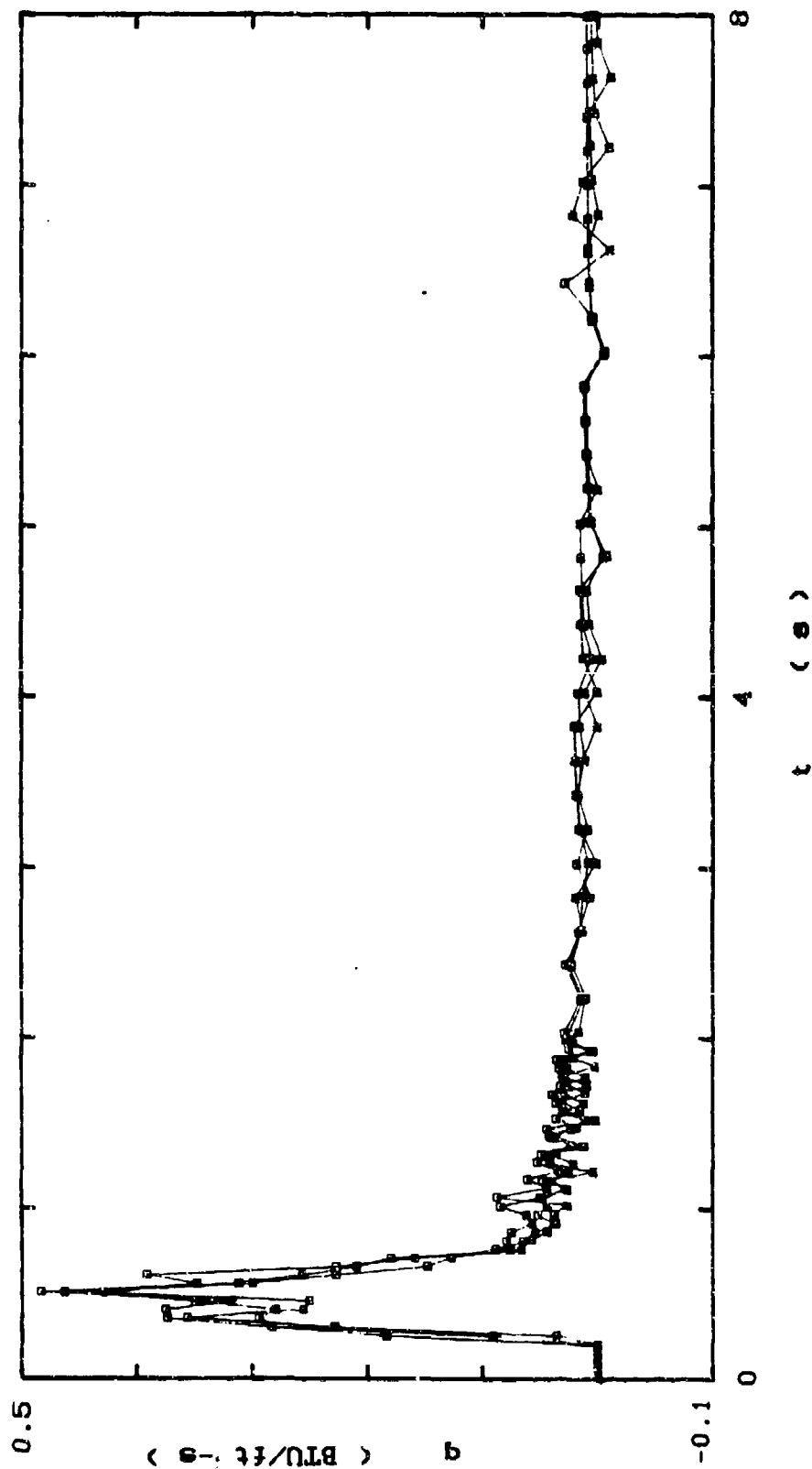Figure 4-3   Calibration Curves for 2D Effects in Thin-film Gages

Figure 4-4   Heat Flux Curves Used In Determining
Experiment Repeatability

highest heat flux levels seem to continue decreasing after the initial transients. Because these levels produced an appreciable surface temperature change (near 10 F), the heat flux was no longer a constant and was expected to decrease. As a result, no correction was employed to account for two-dimensional effects.

To ensure that the main experiment was repeatable, three preliminary runs were made with the gages mounted in the tank. The results of one of the gages is shown in Figure 4-4. The three traces were nearly identical: the slight variations due largely to the slightly differing initial pressures in the tank. Although convinced of the repeatability of the experiment, one gage was maintained in the same location throughout all subsequent runs to ensure that this assumption remained valid.

Test Procedure

Before a test was made, the electronics were given at least 20 minutes to warm up, allowing all transients to die out. The tank was then evacuated to the capacity of the vacuum pump; this was between 2 and 3 psia. During the evacuation, atmospheric pressure and temperature were recorded. After that, the bridge circuits were balanced, and the digital recorder was checked to ensure that the settings employed were the correct ones. The first five channels of the recorder were used for the five heat flux gages, the

22

sixth for the pressure transducer, and the remaining two went unused. The recorder was set to trigger from any change in the pressure tranducer since, from earlier tests, it seemed to have to fastest response. The digital recorder was also set to record data for 8 seconds.

Once the tank had been evacuated, the valve between it and the pump was closed; then, the pump was turned off. The recorder was armed and the tank stopper lever was pulled down sharply to ensure a rapid openning. After the 8 seconds were over, each of the recorded channels was displayed on an oscilliscope. The image was then enlarged and expanded using the controls on the recorder. This was done to facilitate the future digitization of the photograph. Because previous tests indicated that the significant heat transfer occurred within the first 4 seconds, only this portion of the signal was photographed. To take the pictures, the grid on the oscilliscope was illuminated and the intensity of the trace made slightly brighter than the grid. The camera was set with a shutter speed of 1/30 second and an f-stop of 4. Each photograph was marked with an identifying code immediately after processing. This code was used to identify the gage and tank position for that particular trace. Figures 4-5 and 4-6 are sample photographs of a heat flux trace and pressure trace, respectively.

At a later date, the photographs were digitized using a Hewlet-Packard plotter/digitizer. Because the computer to be used in the data reduction could not be made to communicate with the digitizer, data from the digitizer had to be entered manually into the computer. This was the most laborious task of the experiment and was also a driving factor in limiting the recorded signal time to 4 seconds.
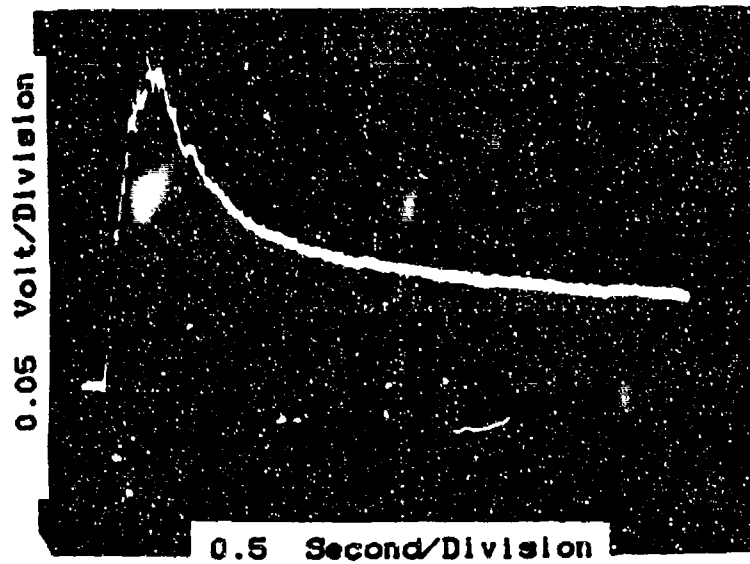
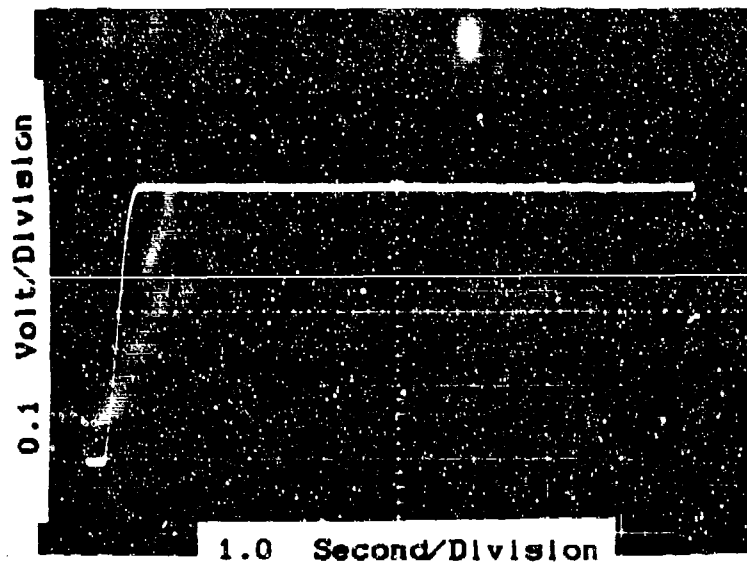Figure 4-5   Sample Oscilliscope Output from Thin-film Gage

Figure 4-6   Sample Oscilliscope Output from Pressure
Transducer

V. Data Reduction

General Comments

From the five different tests needed to accumulate data
from all 19 locations on the tank, average initial conditions
were calculated and used in all data reduction.
The initial conditions used were

$$P_o = 2066.65 \quad \text{lbf/ft}^2 \qquad 0.6\ \%$$
$$P_1 = 200.365 \quad \text{lbf/ft}^2 \qquad 1.3\ \%$$
$$T_o = 540 \qquad R \qquad 0.9\ \%$$

The numbers in the far right column indicated the largest
percentage difference from the average.

In all subsequent calculations, numerical derivatives
were calculated using a centered difference formula for
interior points or a three-point formula for end points. For
any integrations, cubic splines were fit to the data points
and the resulting cubic polynomials integrated exactly.

Measured Data

One of the first quantities calculated from the measured
data was the mass in the tank as a function of time. The
only data needed for this calculation was the transient
pressure data and the initial conditions. Because the
entrance to the tank was a simple converging nozzle,
isentropic relations could be used to calculate the mass flow
as a function of the pressure in the tank. In terms of Mach

number at the throat, the mass flow through the nozzle is
given by [6:84-85]

$$\dot{m} = P_O A M (\gamma/RT_O)^{1/2} [1 + M^2(\gamma-1)/2]^{(\gamma+1)/2(1-\gamma)} \quad [5-1]$$

For a perfect gas under isentropic conditions, the Mach
number can be replaced with the following expressions.

For unchoked flow,
$$M = [2/(\gamma-1)]^{1/2} [(P/P_O)^{(1-\gamma)/\gamma}-1]^{1/2}$$

$$[5-2]$$

For choked flow,
$$M = 1$$

P is the pressure within the tank and P_O is the atmospheric
pressure. Substituting [5-2] into [5-1] and letting $P^+ = (P/P_O)^{(1-\gamma)/\gamma}$ yields the following.

For unchoked flow,
$$\dot{m} = P_O A [2 /([\gamma-1]RT_O)]^{1/2} [P^+-1]^{1/2} P^{+(\gamma+1)/2(1-\gamma)}$$

$$[5-3]$$

For choked flow,
$$\dot{m} = P_O A (\gamma/RT_O)^{1/2} [(\gamma+1)/2]^{(\gamma+1)/2(1-\gamma)}$$

According to the measured pressure data, see Figure 5-1, the
nozzle unchoked after 0.18 second, and the pressure in the
tank reached atmospheric pressure after 0.46 second.
Equation [5-3] was integrated numerically from t=0 to t=0.46
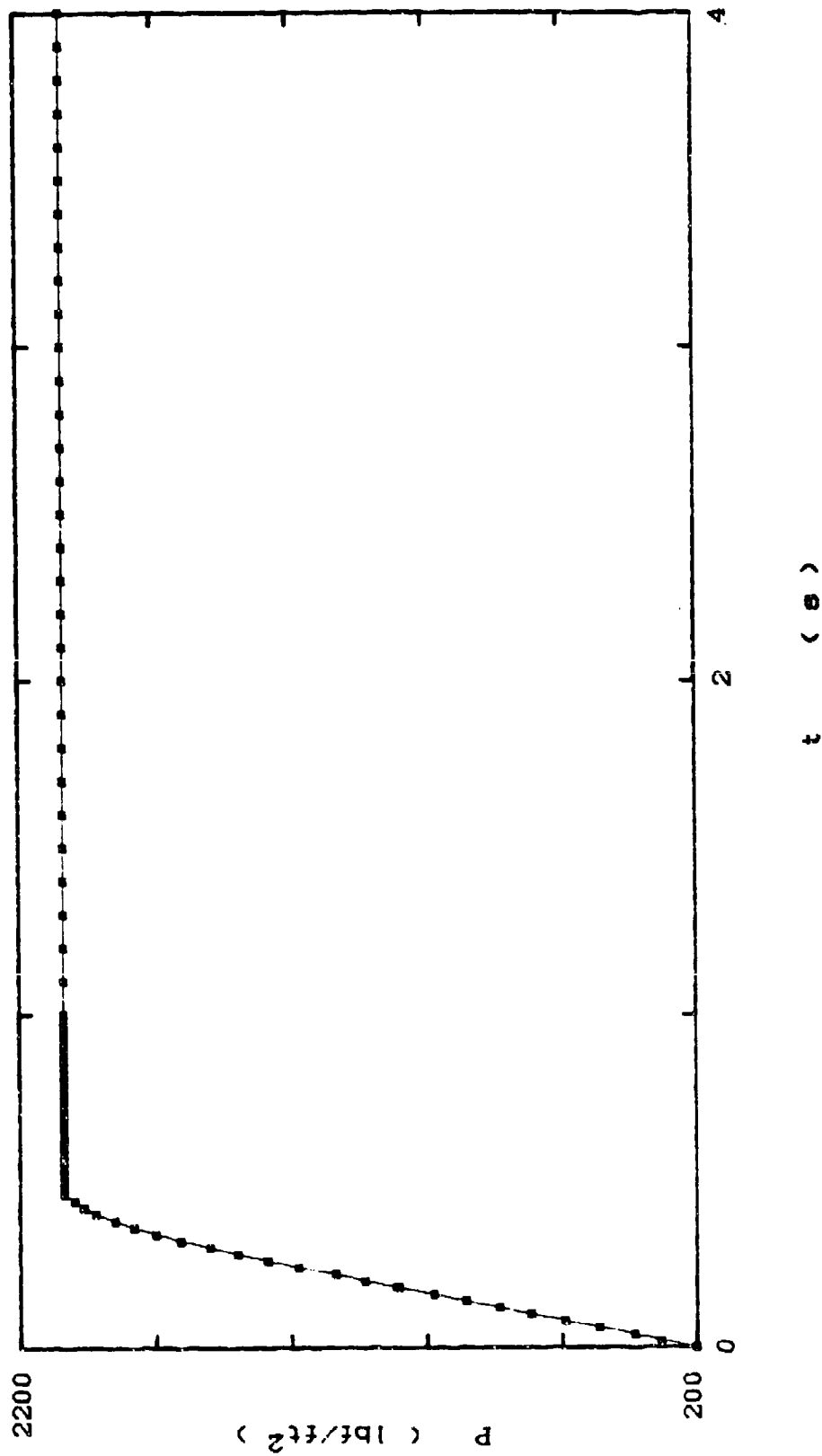second to obtain the mass in the tank as a function of time.

27

Figure 5-1   Pressure Within Tank: 0-4 Seconds

The result is shown in Figure 5-2. It should be noted that
the mass in the tank at 0.46 second, 0.11017 lbm, is somewhat
less than the mass the tank could hold at equilibrium,
0.11749 lbm. This indicated that the temperature of the gas
was still above T_o.

From the pressure data and the newly calculated mass
data, the average temperature of the air within the tank was
found as a function of time. This temperature was found by
using the ideal gas law

$$T(t) = P(t) \, V \, / \, m(t) \, R \qquad\qquad [5-4]$$

The results are plotted in Figure 5-3. Because the partial
derivative of temperature with respect to mass is
proportional to the reciprocal of the mass squared, small
errors in calculating the mass were magnified when the
temperature was calculated. This explains the somewhat
erratic nature of Fig. 5-3. However, the general trend of
increasing temperature is readily apparent.

Next, from the voltage data of the thin-film gages,
surface temperatures were calculated using Eq. [3-3]. These
temperatures were then used in the Cook and Felderman
equation [3-7] in order to determine the surface heat fluxes.
The value for $\rho ck/\pi$ used in this equation was the well
documented value of 0.001819 BTU^2/ft^4-R-s. [3] This data
spanned the time period between 0 and 4 seconds. The heat
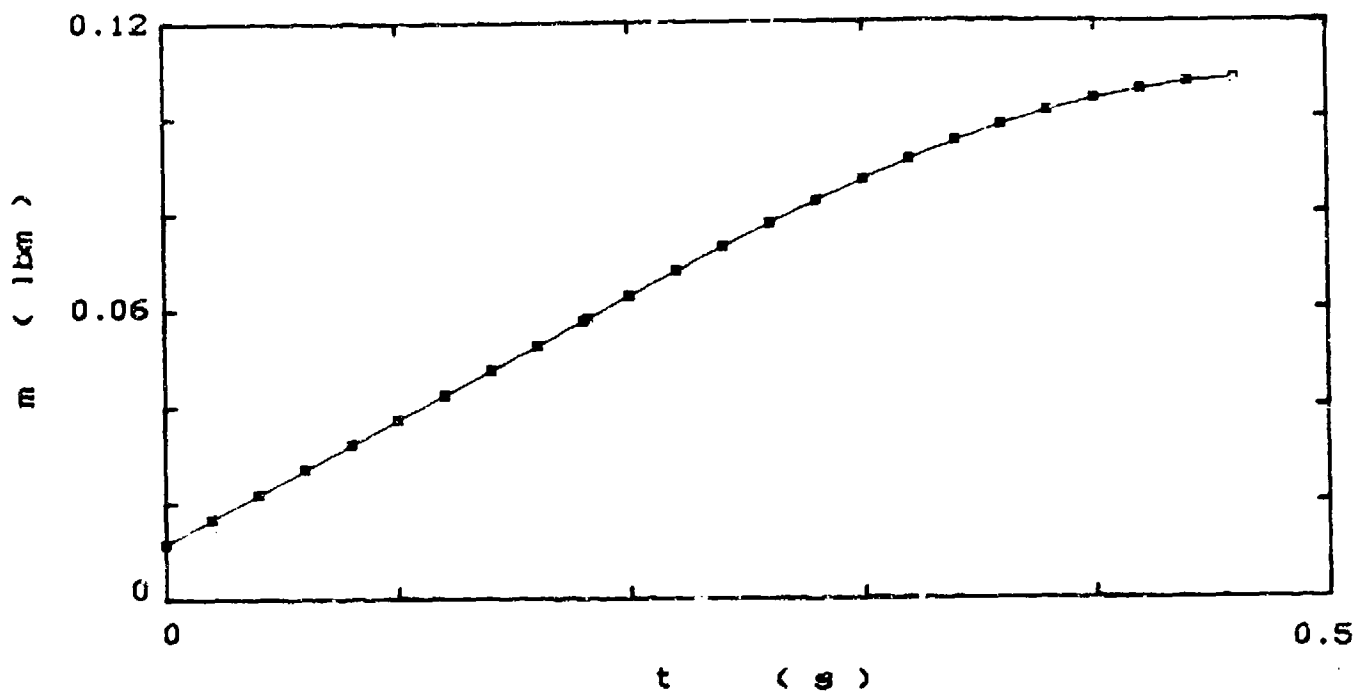flux of each gage was calculated separately, and then it was

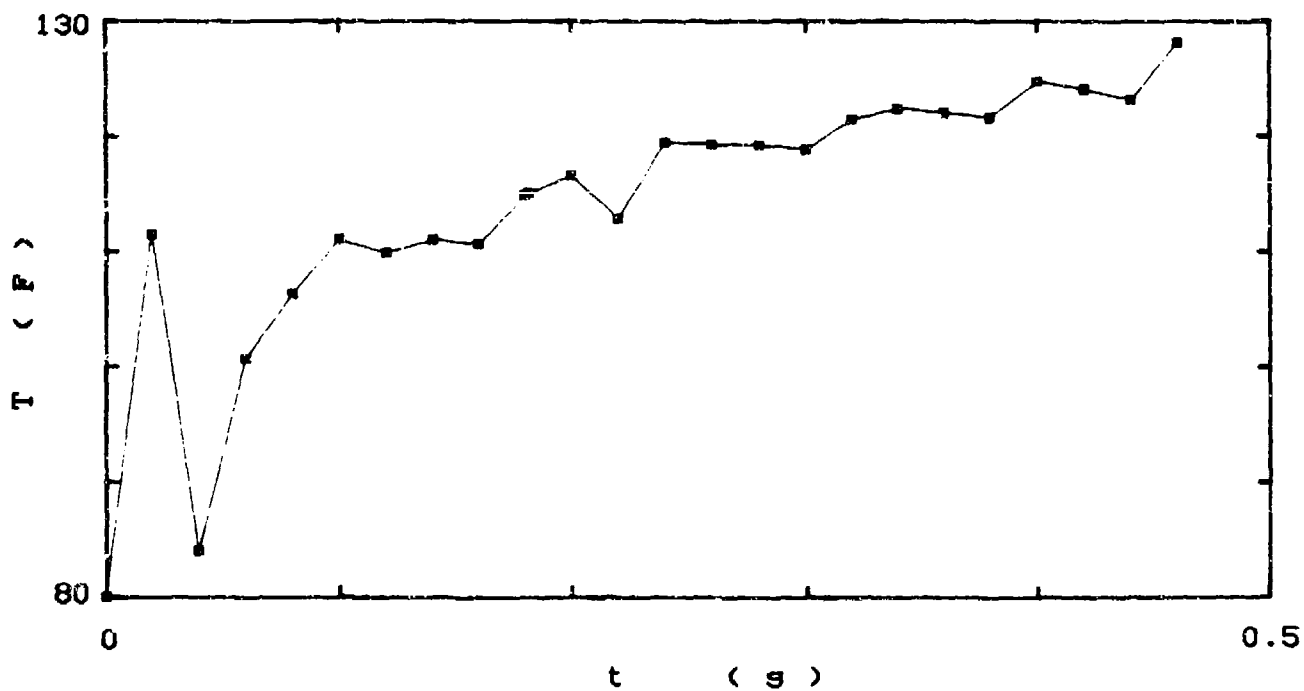Figure 5-2   Mass of Air Within Tank: 0-0.46 Second

Figure 5-3   Average Air Temperature in Tank: 0-0.46 Second

multiplyed by the area of that section of tank it was representing. The results from all the gages were then added together to get the total heating rate for the entire tank. See Appendix B for this information in tabular form. The data was then integrated numerically to determine the heat transferred to the tank walls as a function of time. This data is displayed in Figure 5-4.

At the end of the 4 seconds, the total heat transferred was approximately 80% of the total amount which should have been transferred had equilibrium been reached. That maximum is 3.92 BTU and depends solely on the initial and final tank pressures as well as the volume of the tank. (See Section II: the second classical problem.) As a result, the curve was extrapolated out to 10 seconds to account for the missing energy, but that will be discussed shortly. The heat flux data from the individual gages versus their position in the tank are plotted in Figure 5-5 at specific moments in time. These plots give an indication of the heating distribution along the tank wall.

From the mass, temperature, and heat data, the average internal and kinetic energies of the gas within the tank were calculated. Recall Eq. [2-3],

$$m[c_v T + u^2/2g_c] - m_1 c_v T_o = (m-m_1)c_p T_o - Q$$
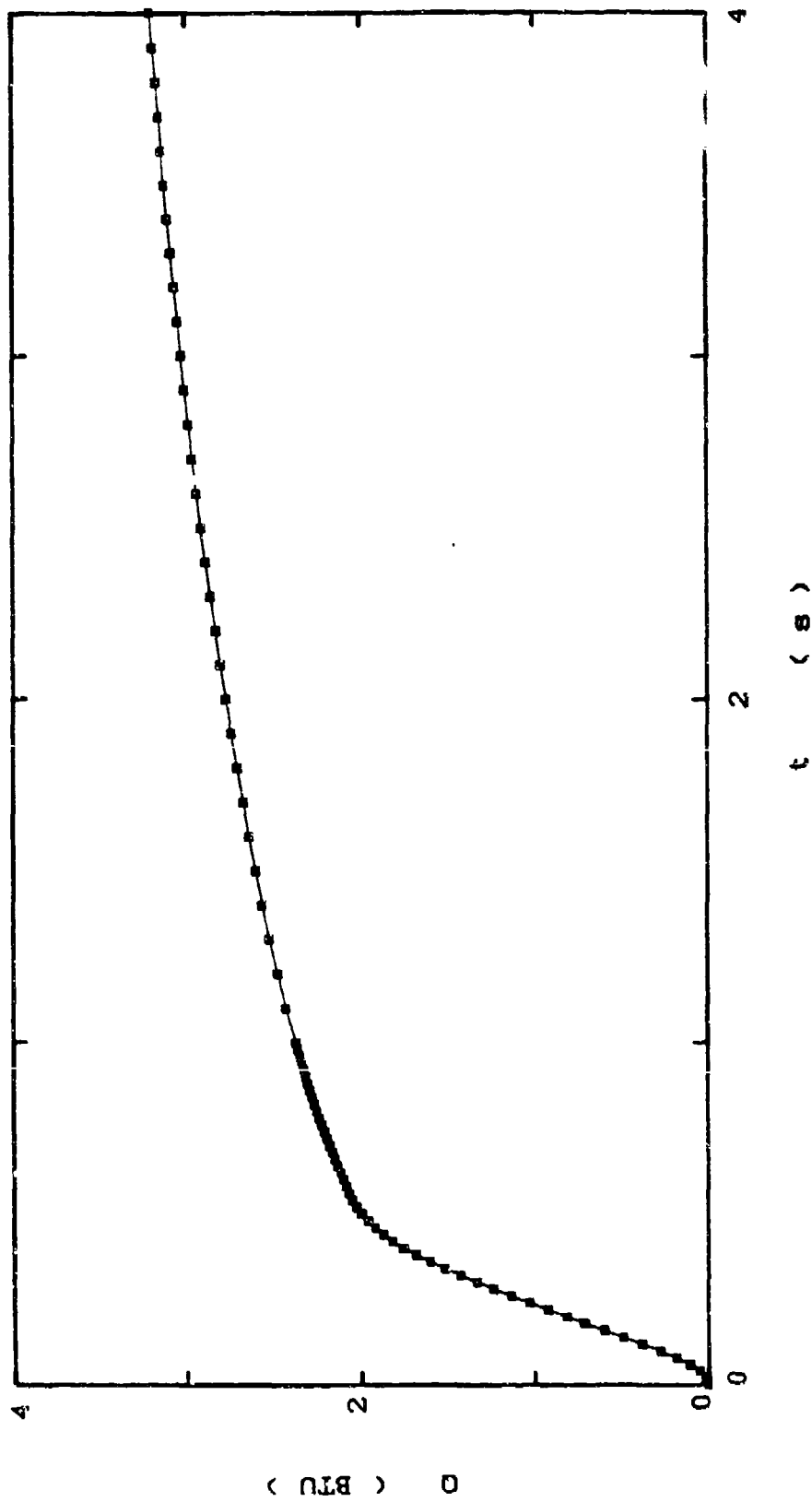
31

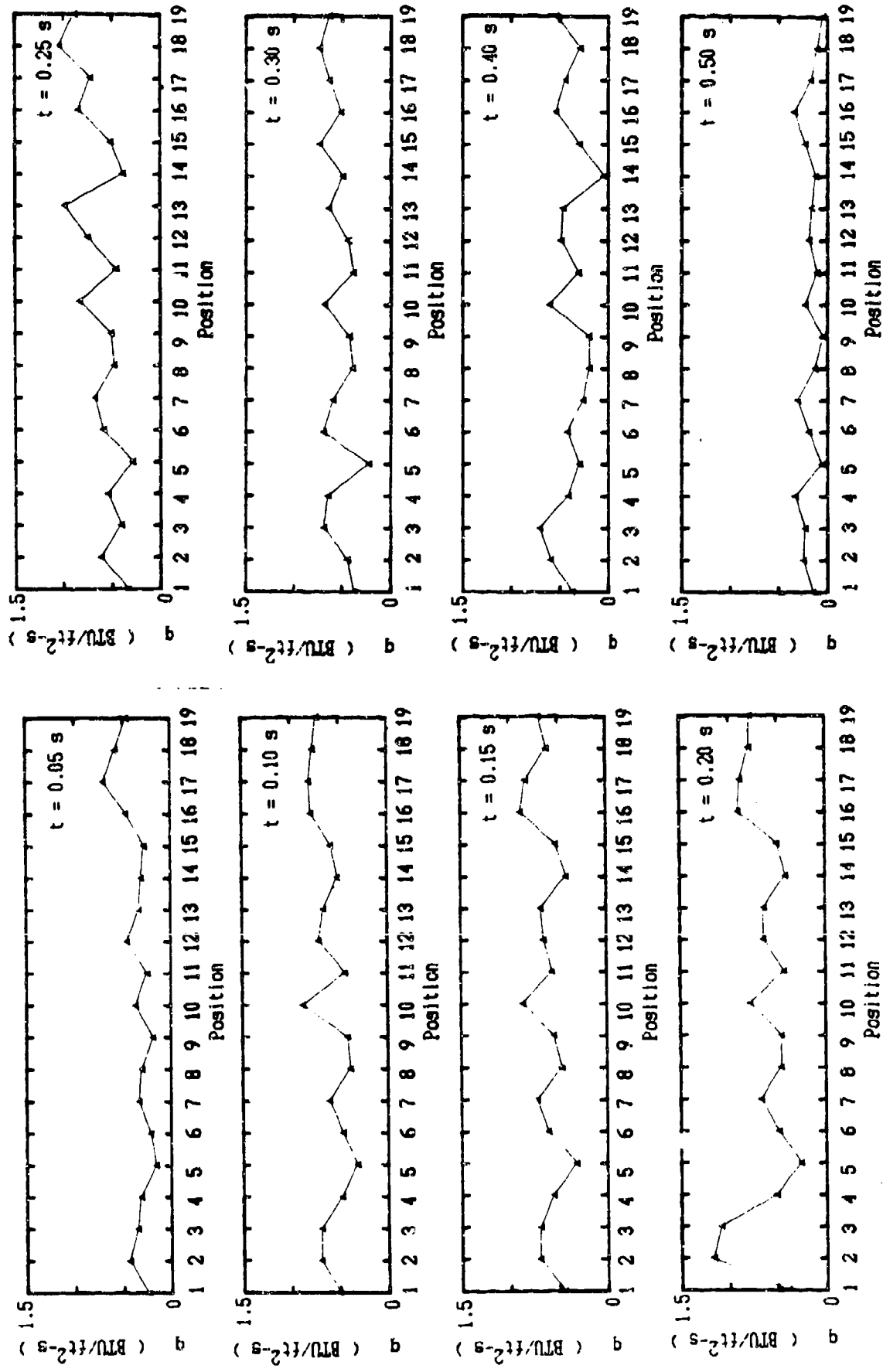Figure 5-4   Heat from Air to Tank Walls: 0-4 Seconds

Figure 5-5   Heat Flux Versus Wall Location

33

Since the only unknown in Eq. [2-3] is the kinetic energy term, $mu^2/2g_c$, it could be determined. Each of the energy terms appearing in Eq. [2-3] is plotted in Figure 5-6.

Because rapid charging involves high-speed flow, the adiabatic wall minus wall temperature difference was chosen as the driving temperature potential for heat transfer. Due to the unknown dynamics of the flow, a recovery factor of unity was chosen for lack of a better estimate. This reduced the driving potential to be the total temperature minus the wall temperature. The total temperature, T^*, is shown in Figure 5-7.

$$T^*(t) = T(t) + [u(t)]^2/2g_c c_p \qquad [5-5]$$

To determine an average convection coefficient for the tank, h(t), the following equation was used.

$$h(t) = q(t) \ / \ [T^*(t) - T_o] \qquad [5-6]$$

To get q(t), the data for Q(t) was divided by the total surface area of the tank and numerically differentiated. The plot of h(t) is shown in Figure 5-8. Anticipating a relationship between h(t) and Reynolds number, log(h) was plotted versus the log(ρu). The velocity, u, was determined from the kinetic energy data. This logarithmic plot is shown in Figure 5-9.
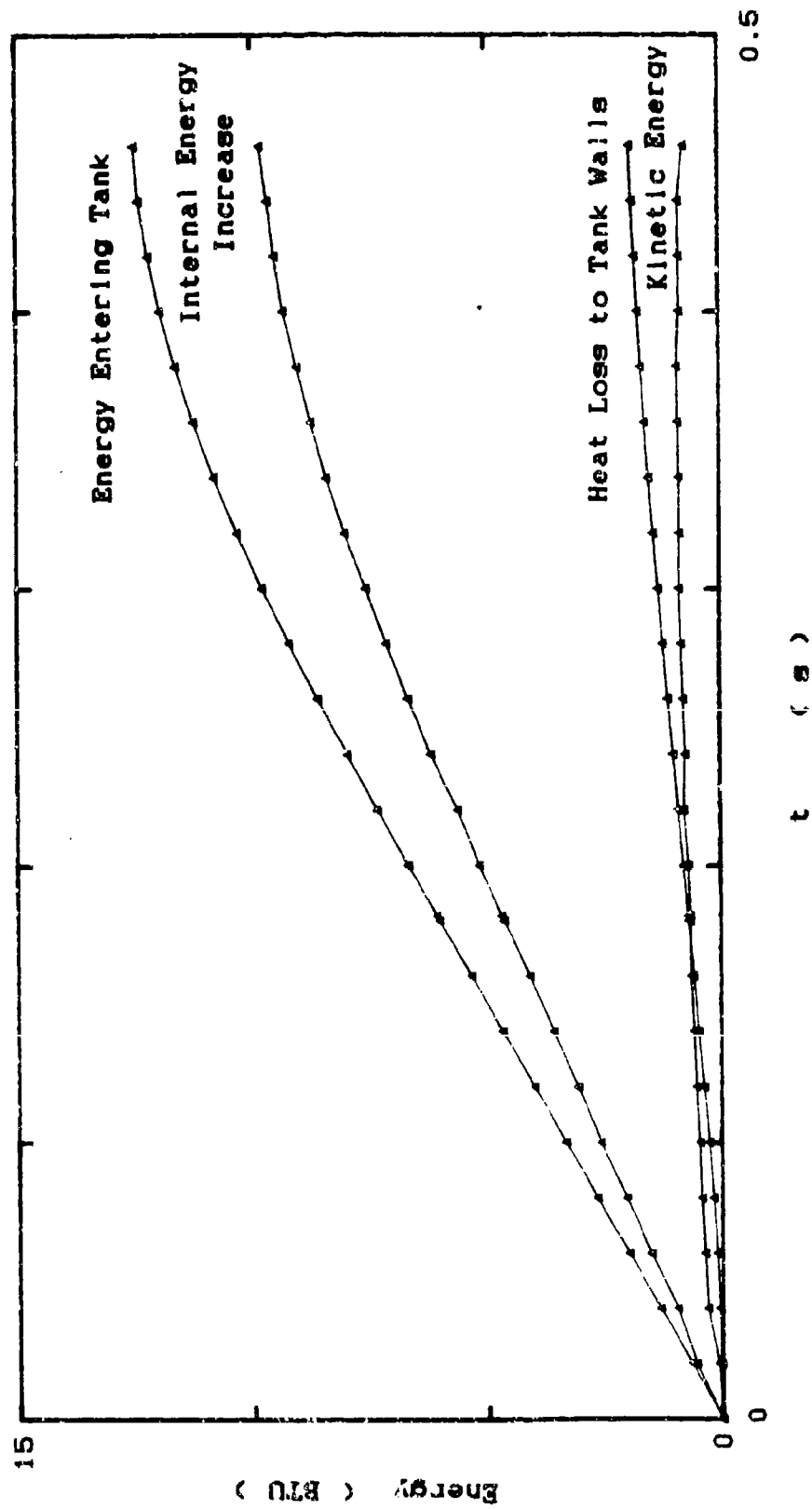
34

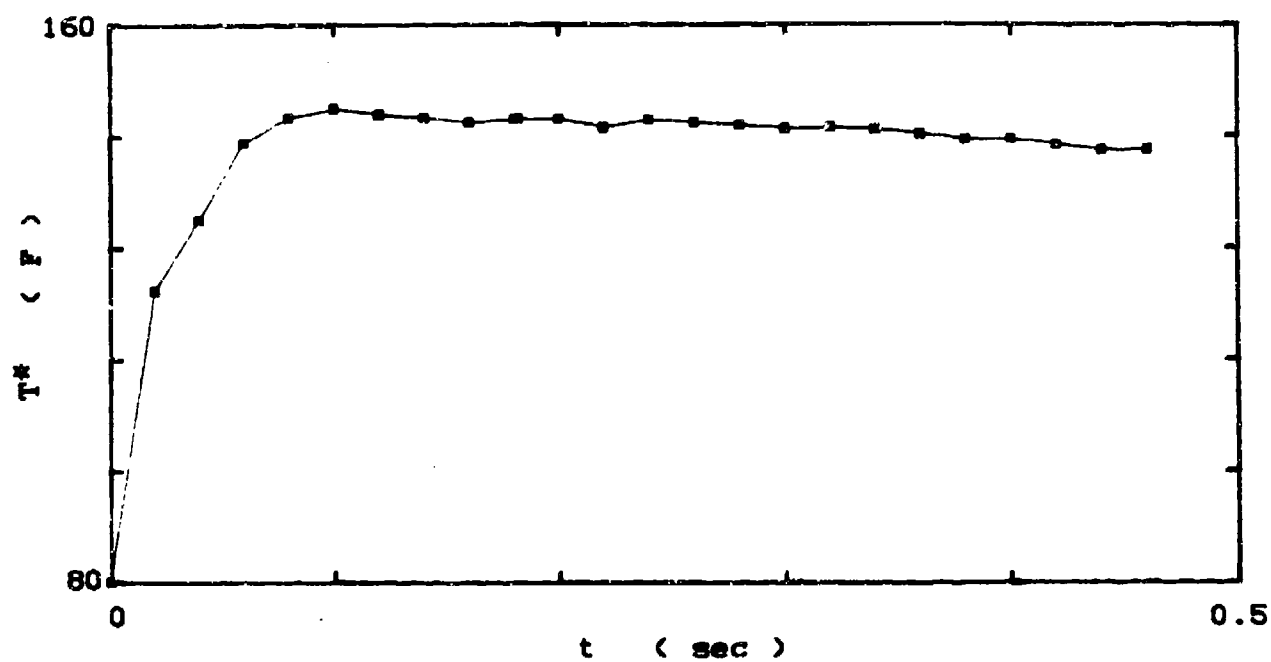Figure 5-6   Terms in the Energy Balance of Eq. [2-3]:
0-0.46 Second

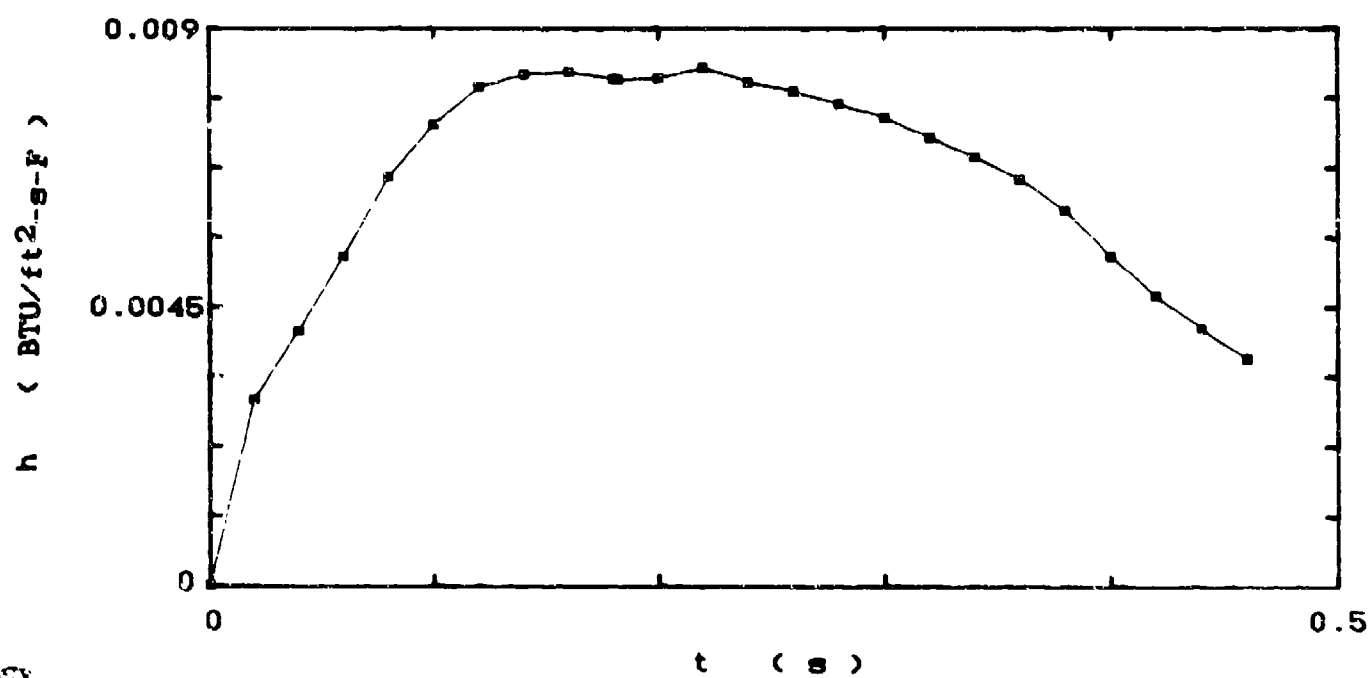Figure 5-7   Average Total Air Temperature: 0-0.46 Second

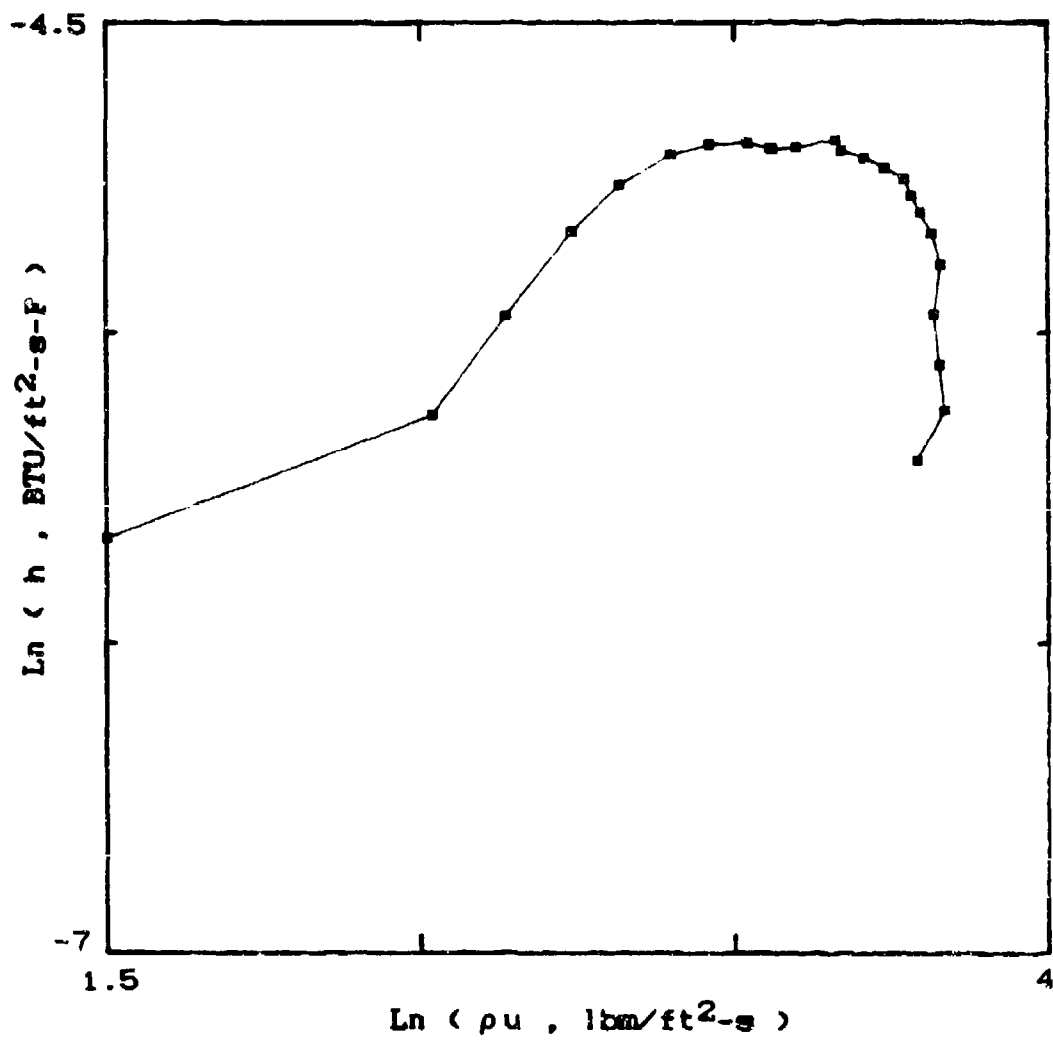Figure 5-8   Average Convection Coefficient: 0-0.46 Second

Figure 5-9   Ln (h)   Versus   Ln (ρu) :   C-0.46 Second

Extrapolated Data

Because the heat transferred after 4 seconds was short
of the theoretical equilibrium value, an attempt was made to
account for this energy by extending the time for equilibrium
to be established. After several attempts, 10 seconds was
found to be the time at which the heat transfer was completed
and at the maximum value. In order to extrapolate all the
data out to 10 seconds, three quantities had to be chosen as
independent variables. Since the pressure within the tank
was known, it was selected as one of the independent
variables. The two other quantities finally chosen were the
convection coefficient, h, and the velocity, u.

The convection coefficient was chosen as an independent
variable because prior trials at extrapolation indicated that
h(t) remained fairly constant after 1 second. Therefore, it
was assumed that from 1 to 10 seconds h(t) = 0.0014385
BTU/ft^2-F-s . This modified curve is displayed in Figure
5-10.

The velocity was also chosen as a known quantity because
there was some theory with which to predict its behavior. The
rate of momentum dissipation of a fluid within a tank depends
upon the force on that fluid due to the shear stress at the
wall. Since the mass changed very slowly after 0.46 second,
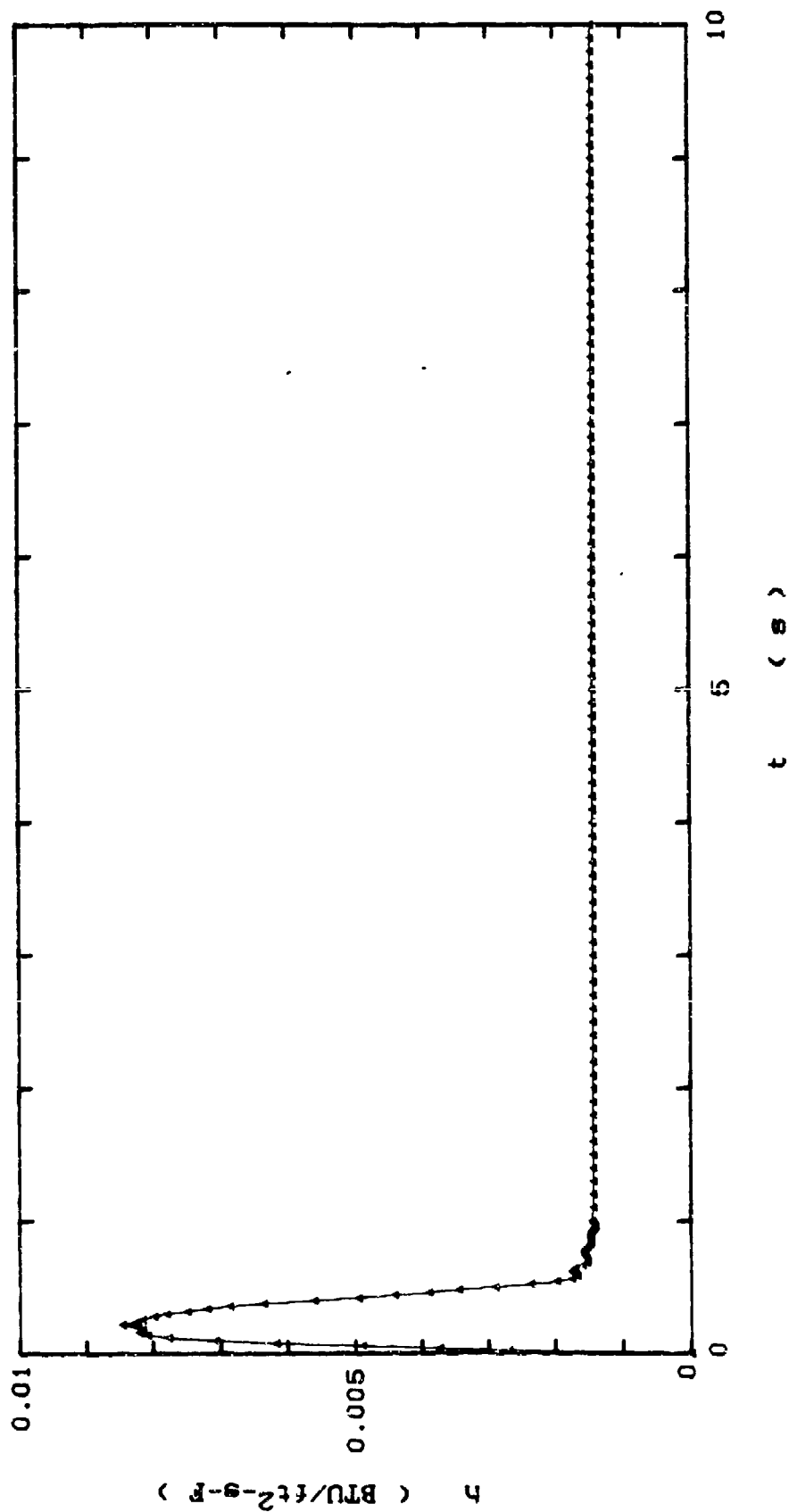it may be approximated as a constant. Doing so, the momentum

Figure 5-10   Modified Average Convection Coefficient:
0-10 Seconds

dissipation may be expressed as

$$d(mu(t))/dt = -\tau_w A_{surface} = -\mu u(t)A_{surface}/L \quad [5-7]$$

After integration,

$$u(t) = u(0.46) \exp (-(\mu A_{surface}/mL)(t-0.46)) \quad [5-8]$$

Where τ_w, wall shear stress, has been approximated by $\mu u(t)/L$, and L is some characteristic length. From Eq. [5-8], the velocity should decrease exponentially. Because the velocity prior to 0.46 second was calculated from measured quantities, a simple exponential decay was fit to the velocity curve from 0.46 to 10 seconds. The time constant, $1/(\mu A_{surface}/mL)$, was taken to be 0.5 sec in order to have u(10) approximately equal to zero. This curve is shown in Figure 5-11.

To find the mass in the tank as a function of time, the energy equation, Eq. [2-3], can be rewritten in terms of P, h, m, and u.

$$c_v PV/R + mu^2/2g_c - m_1 c_v T_o =$$
$$mc_p T_o - hA(PV/mR + u^2/2g_c c_p - T_o) \quad [5-9]$$

Differentiating with respect to time and solving for m yields

$$\dot{m} = \frac{(mu\dot{u}/g_c) + d[hA(PV/mR + u^2/2g_c c_p - T_o)]/dt}{c_p T_o - u^2/2g_c} \quad [5-10]$$

Equation [5-10] was numerically integrated and the resulting mass function is plotted in Figure 5-12. With the mass in
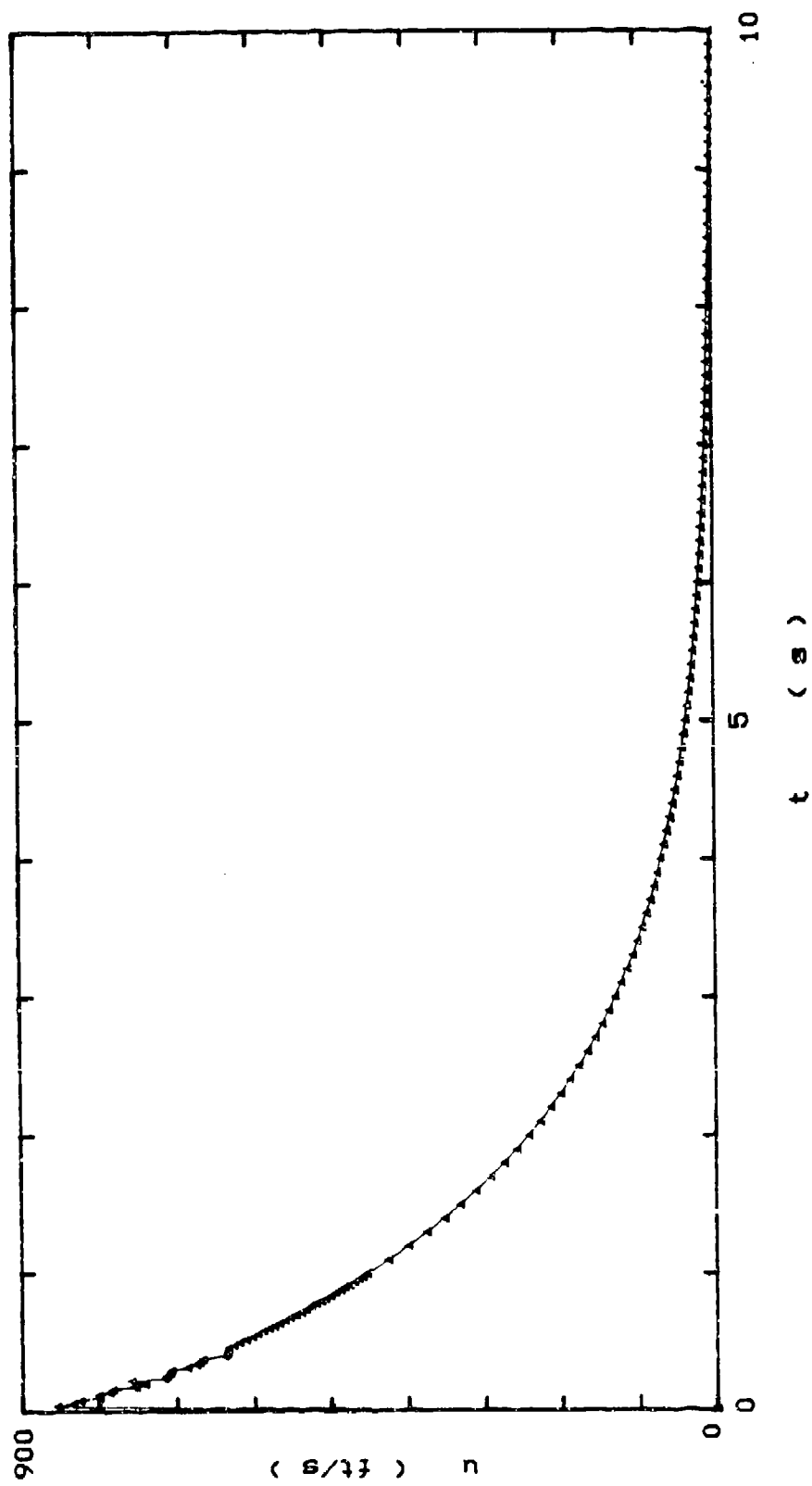
Figure 5-11   Modified Average Velocity: 0-10 Seconds

41

the tank now estimated, the average and total temperatures were found using Eqs. [5-4] and [5-5], respectively. They are shown in Figure 5-13. From this resulting data, the energy terms in Eq. [2-3] were calculated. They are displayed in Figure 5-14. Also, the plot of log(h) versus log(pu) was found and is shown in Figure 5-15.

To verify that the second law of thermodynamics was not violated as a result of the modified data, each of the three terms of Eq. [2-4] was calculated from the estimated data. As a convenience, entropy per unit mass was taken to be zero at atmospheric conditions. This eliminated the need to calculate the ms_0 term.

The tank wall temperature was taken to be T_0 since the wall had such a large heat capacity and the heat flux was so small. In fact, for a constant heat flux applied to the boundary of a semi-infinite solid, the ratio of temperature change for a stainless steel solid (tank wall) to that of a quartz solid (thin-film gage) is given by

$$\Delta T_{tank} / \Delta T_{gage} = (\rho ck)_{gage} / (\rho ck)_{tank} \qquad [5-11]$$

For the material properties involved, this ratio is approximately 0.2. Since the maximum gage temperature differences were between 3 and 5 F, the maximum temperature change of the tank wall would be about 1 F. Thus, the wall temperature was assumed to remain constant at T_0.

To calculate $\dot{S}_{c.v.}$, Eq. [2-5] was used.

42
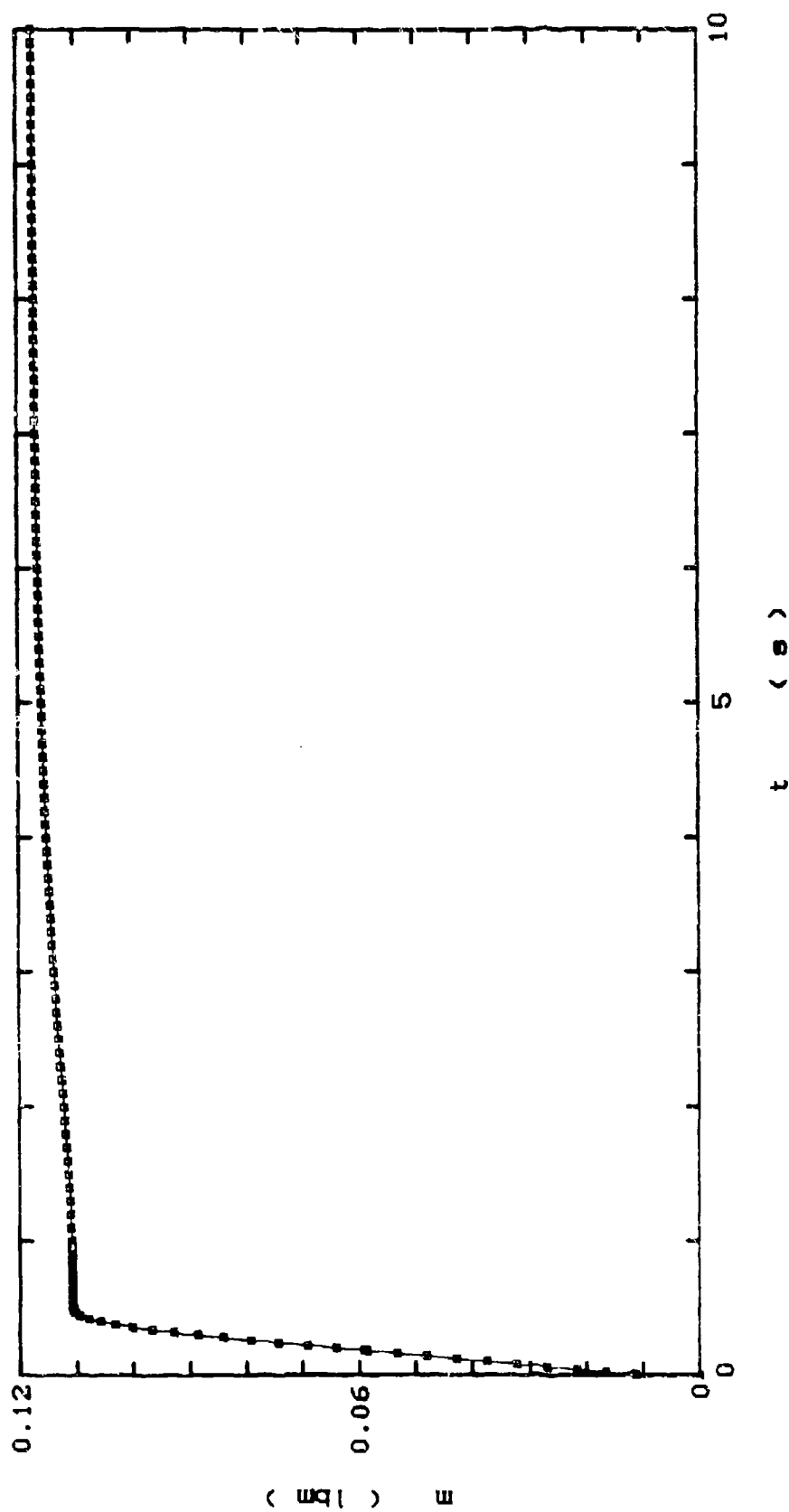
Figure 5-12   Extrapolated Mass in Tank: 0-10 Seconds
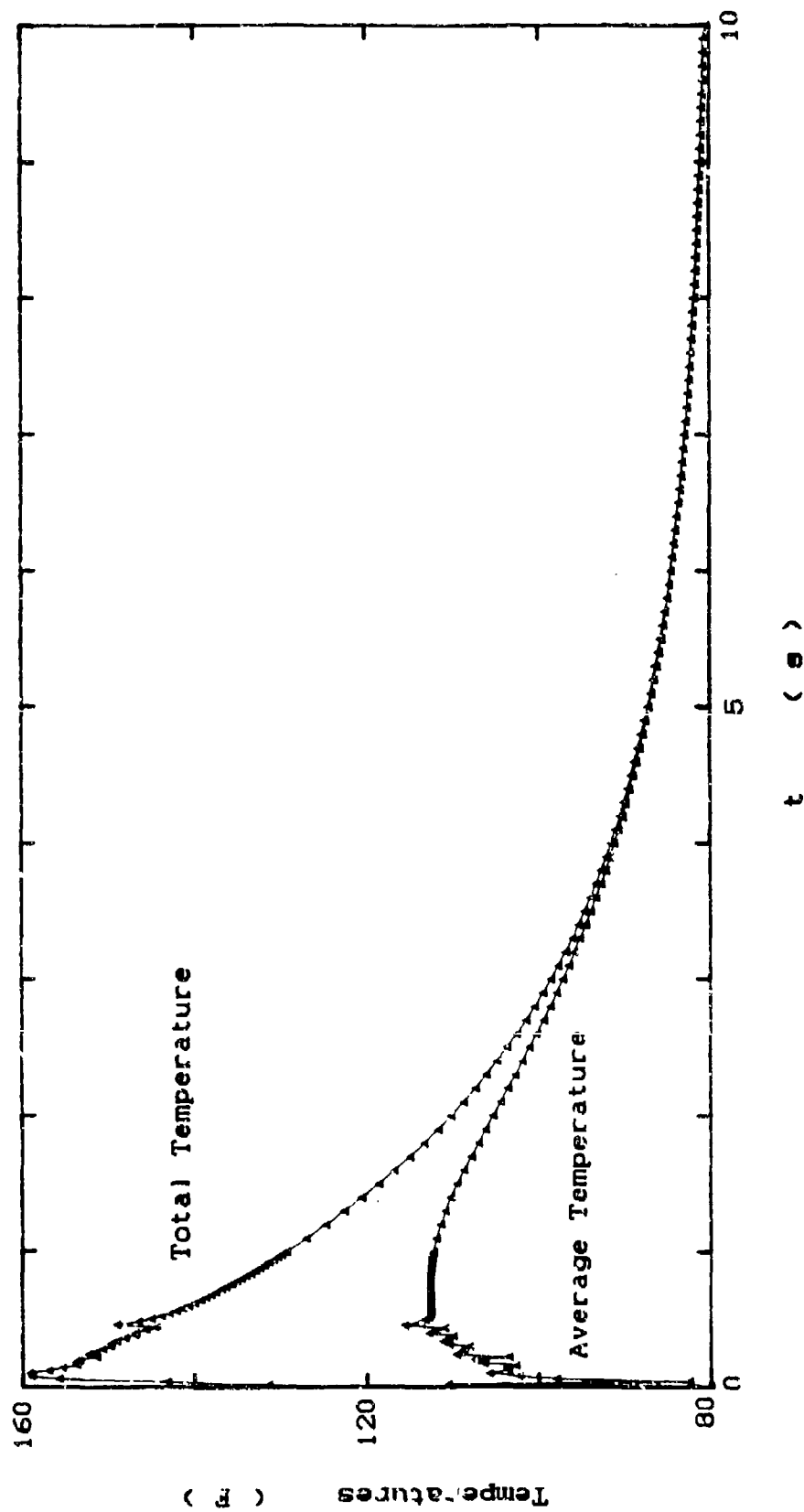
Figure 5-13 Extrapolated Average and Total Temperatures:
0-10 Seconds

44
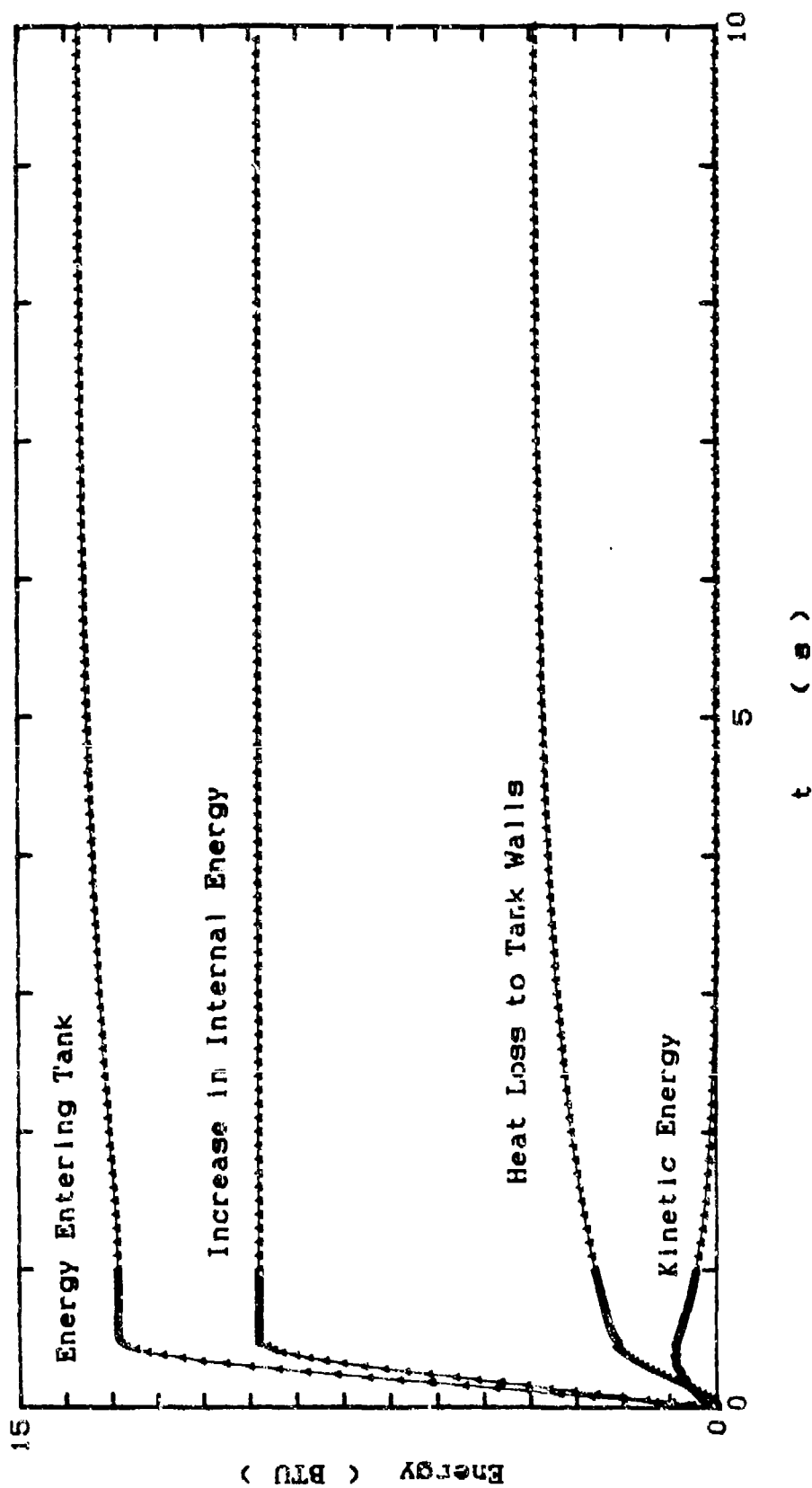
Figure 5-14 Extrapolated Terms in the Energy Balance of Eq. (2-3): 0-10 Seconds

45
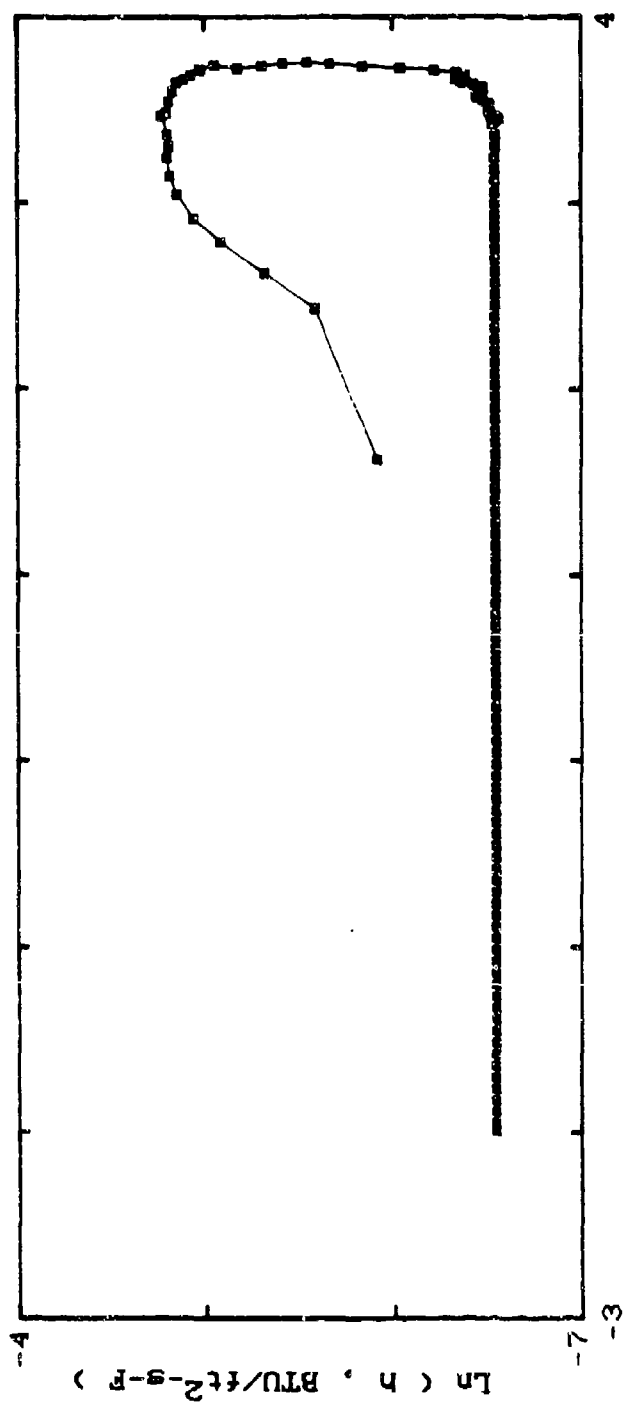
Figure 5-15   Ln (h) Versus Ln (ρu) :   0-10 Seconds

$$s(t) = c_p \ln[T/T_o] - R \ln[P/P_o] \qquad [5-12]$$

Thus,

$$S_{c.v.}(t) = m(t)s(t)$$

or, $\qquad\qquad\qquad\qquad\qquad\qquad\qquad\qquad\qquad$ [5-13]

$$\dot{S}_{c.v.}(t) = d(m(t)s(t))/dt$$

The results of these calculations are shown in Figure 5-16.
Recall that $s_o = 0$. Equation [2-4] then requires that

$$\dot{S}_{c.v.}(t) + \dot{Q}/T_o \geq 0 \qquad [5-14]$$

Figure 5-17 shows the sum of these entropy terms, and indeed,
the sum is initially greater than and quickly approaches
zero.
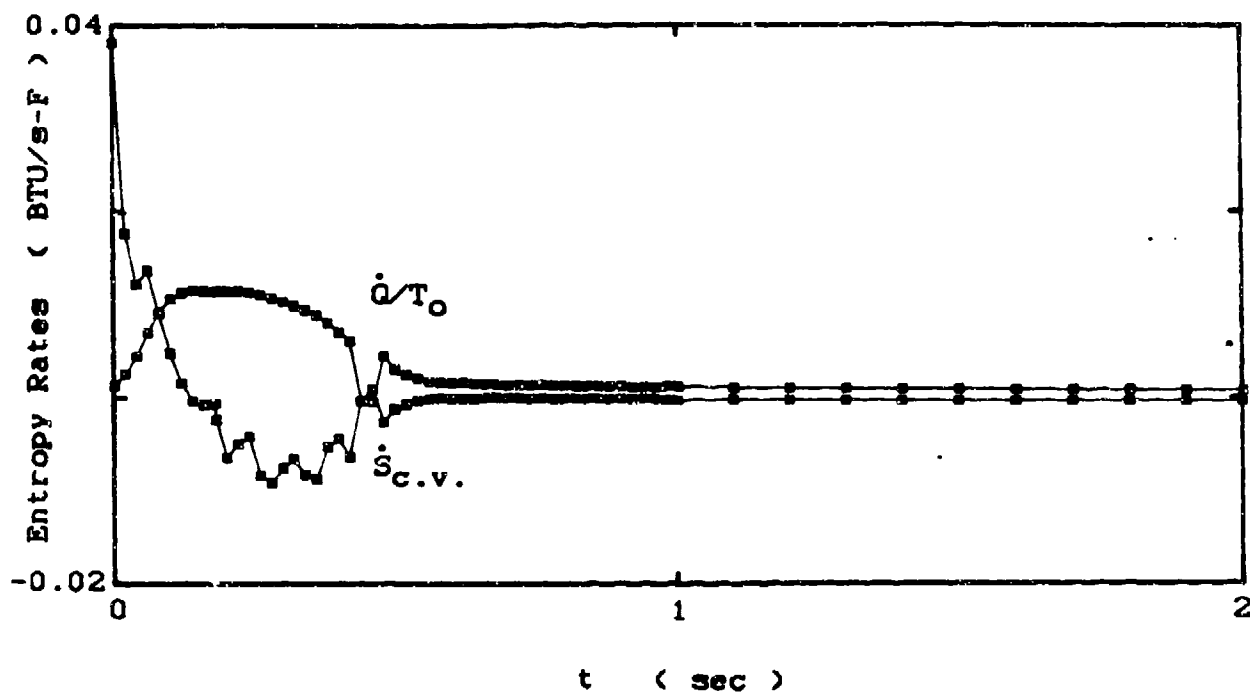
Figure 5-16   Entropy Entering, Leaving, and Stored in Tank:
0-2 Seconds
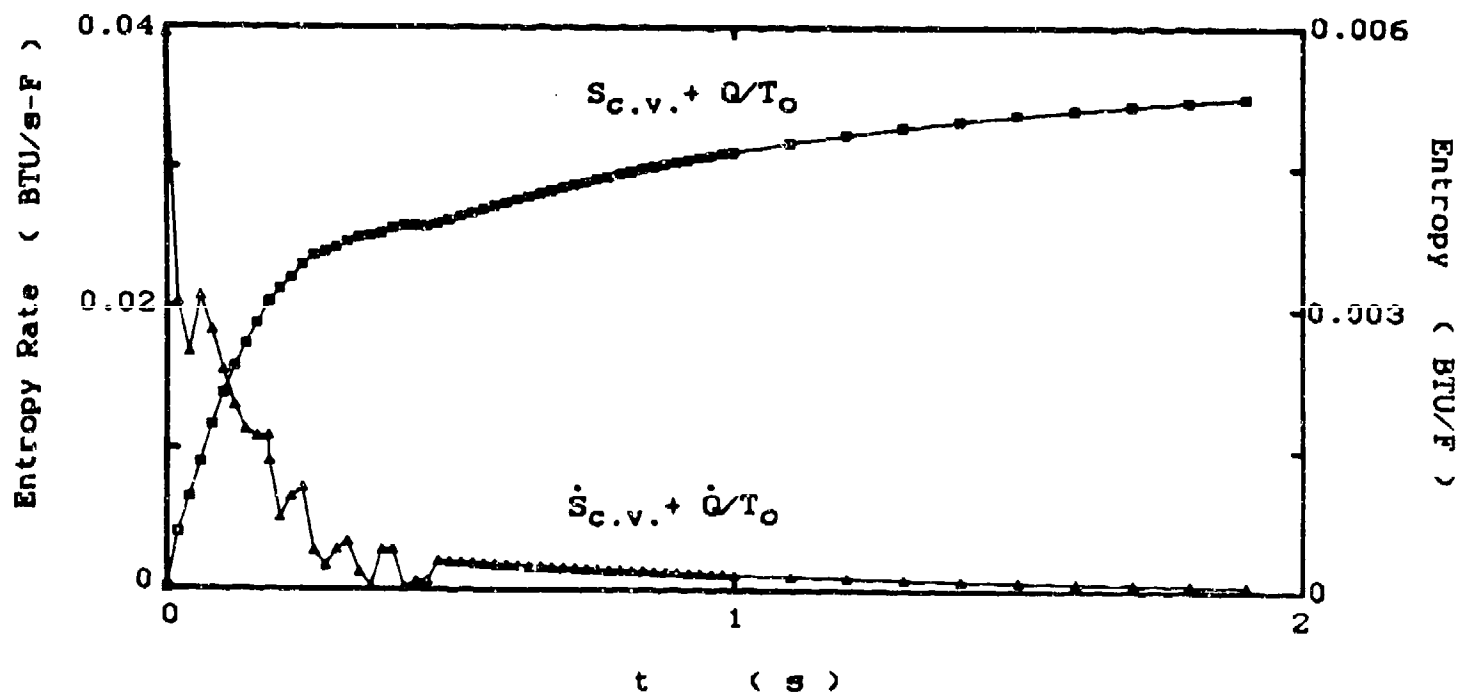
Figure 5-17   Sum of Entropy Terms from Fig. 5-16:
0-2 Seconds

48

VI. <u>Results</u>

As shown in Figure 5-5, the heat flux level along the
tank wall at any given time is fairly uniform. Deviations do
exist, however, and may imply recirculation regions within
the tank. With the exception of the positions on the bottom
of the tank, the crests in heat flux remain crests and the
troughs remain troughs. What may be happenning in the tank
is this: the instant the tank is opened, air flowing out of
the choked nozzle expands immediately into the upper corners
of the tank. The flow then continues down the tank and
finally stagnates at the base. As the tank fills, the flow
out of the nozzle becomes more jet-like and swirling begins.
This swirling seems to reach a peak around the time at which
the nozzle unchokes. After that time, the velocity of the
entering air decreases as does the kinetic energy of the air
within the tank. The flow pattern during the time of maximum
swirling may appear as that shown in Figure 6-1.

From all the figures in Section V, it's clear that the
bulk of the charging process is over in a very short time.
The pressure within the tank rose to atmospheric pressure in
0.46 second. The mass nearly rose to its maximum value in
0.46 second. From that time on, mass slowly entered the tank
as the average gas temperature within gradually decreased.
After 0.46 second, slightly over 50% of the heat energy had
already been transferred from the gas to the tank walls. By
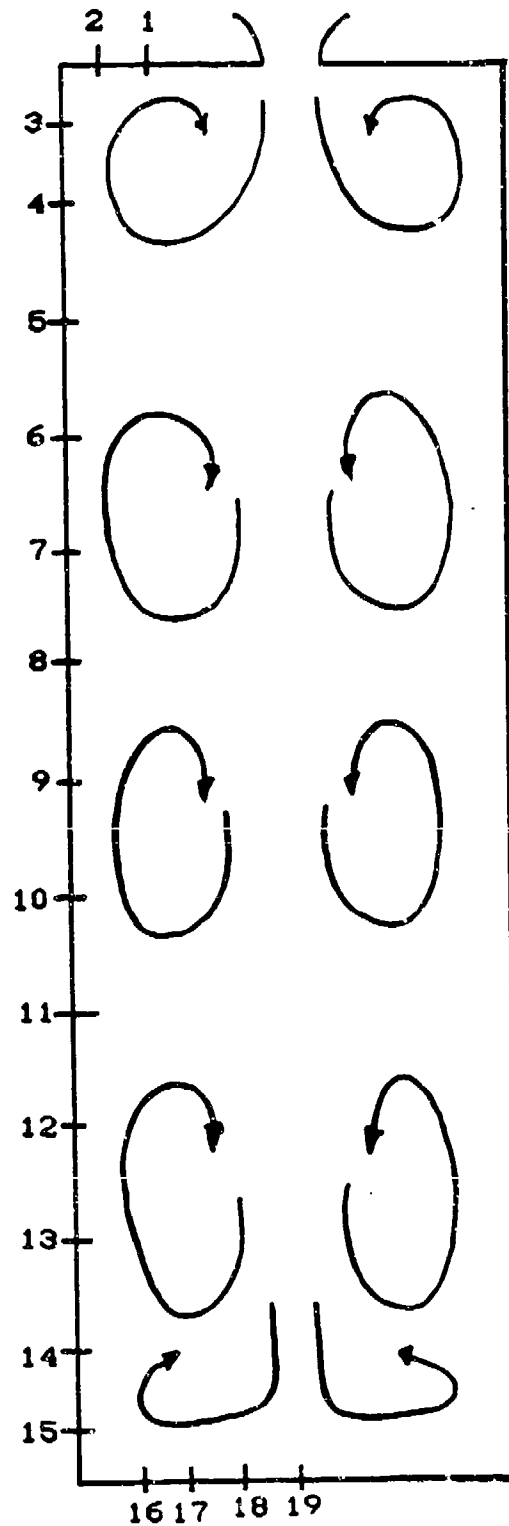
Figure 6-1   Possible Flow Pattern During Charging

four seconds, 80% had been transferred; by 8 seconds, 95%; and by 10 seconds, almost 100%.

A convection coefficient was derived and plotted in Figure 5-10. This h(t) was also plotted on a log scale and is shown in Figure 5-15. The plot contains the same strange behavior as the plot in Fig. 5-9. This data indicates a complex flow pattern within the tank with two, possibly three, different regimes. During the early times of the process, h is proportional to $(\rho u)^{1.114}$. A transition then occurs and h seems to be independent of (ρu). The third flow pattern is the straight line in the plot and is a result of choosing h(t) to be constant after 1 second. Little can be said concerning the meaning of that portion of the curve. Because of this strange behavior, it was not possible to establish a relationship between h(t) and Reynolds number.

This erratic behavior of the convection coefficient also precluded its use as a tool for predicting heating rates in other tanks. Another approach was needed. To this end, the heating rate for the entire tank, $\dot{Q}(t)$, was found from differentiating Q(t) and is displayed in Figure 6-2.

$\dot{Q}(t)$ depends upon the initial pressure conditions, the volume of the tank, and the size of the inlet. Also, it will depend upon the time during which the nozzle is choked and the time for pressure within the tank to equalize with the ambient pressure. These factors were considered in extending the measured results to other tanks with conducting walls
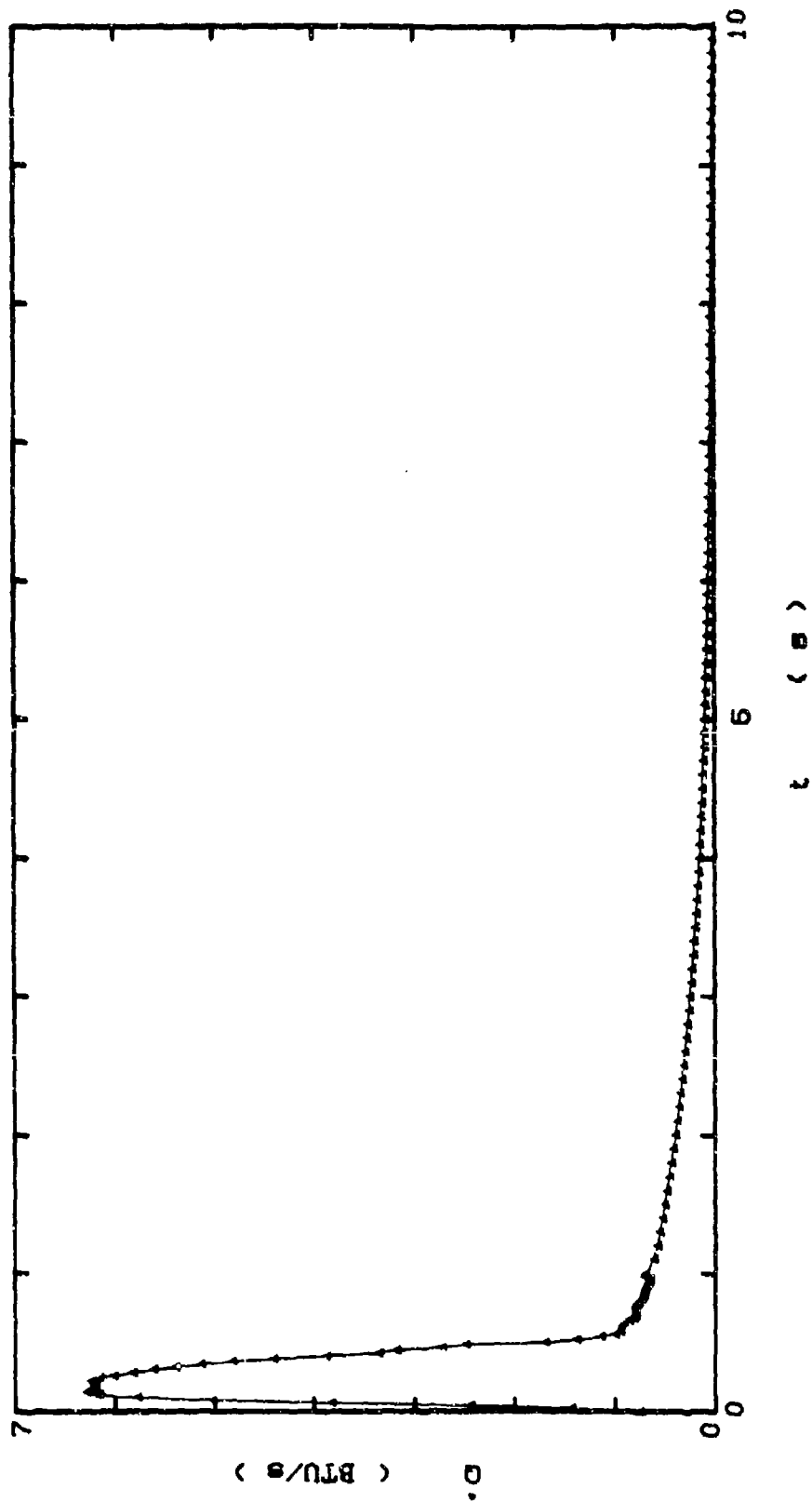
Figure 6-2: Heating Rate of Tank Wall: 0-10 Seconds

which have roughly the same thermal properties as stainless steel. Those properties are $\alpha = 0.147$ ft^2/hr and $\rho ck = 435$ BTU^2/ft^4-hr-F^2. It should be noted here that the following calculations (with the exception of Q_{tot}) are only estimates.

As was discussed previously, the total heat transferred from the gas to the tank walls is just the total flow work done on the gas. This energy, Q_{tot}, equals the difference in initial pressures multiplied by the volume of the tank. This relationship is plotted in Figure 6-3 for various heat levels.

To find the time at which the nozzle unchokes as well as the time at which the pressures equalize, the measured pressure curve was represented by two straight lines. The first line describes the pressure rise while the nozzle is choked. Since this relationship is a linear one, no approximation needs to be made. The second line represents the pressure rise between the time from the unchoking of the nozzle to the time the tank pressure reaches P_o. This is an approximation to the actual curve. See Figure 6-4. The slopes of these lines were calculated from the measured data, and they yielded the following results.

$$t_{uc} = (0.52828P_o - P_1) / 4952.25$$

[6-1]

$$t_p = t_{uc} + (1 - 0.52828) P_o / 3481.71$$

53
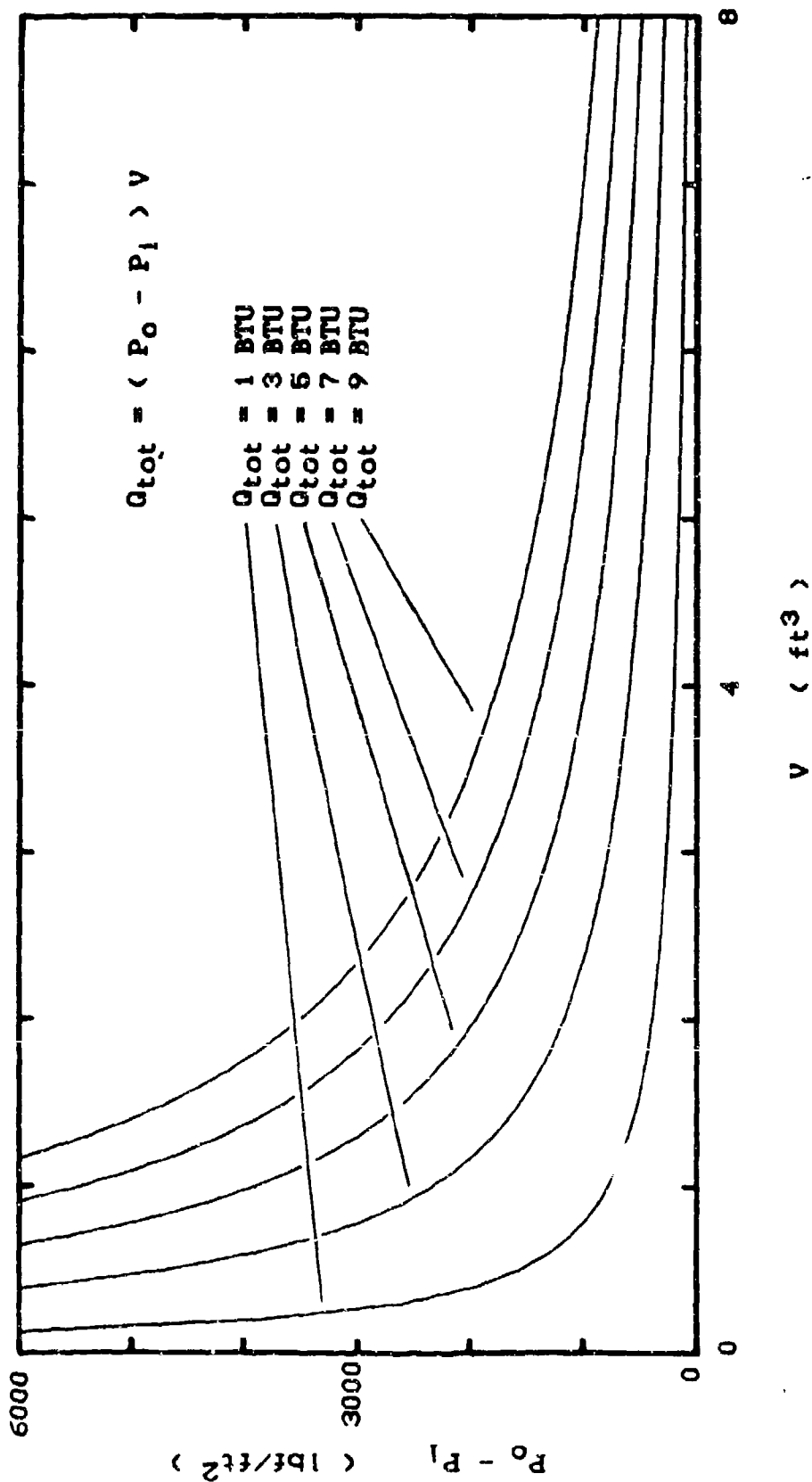
Figure 6-3   Relationship Between Pressure Difference,
Tank Volume, and Total Heat Transferred
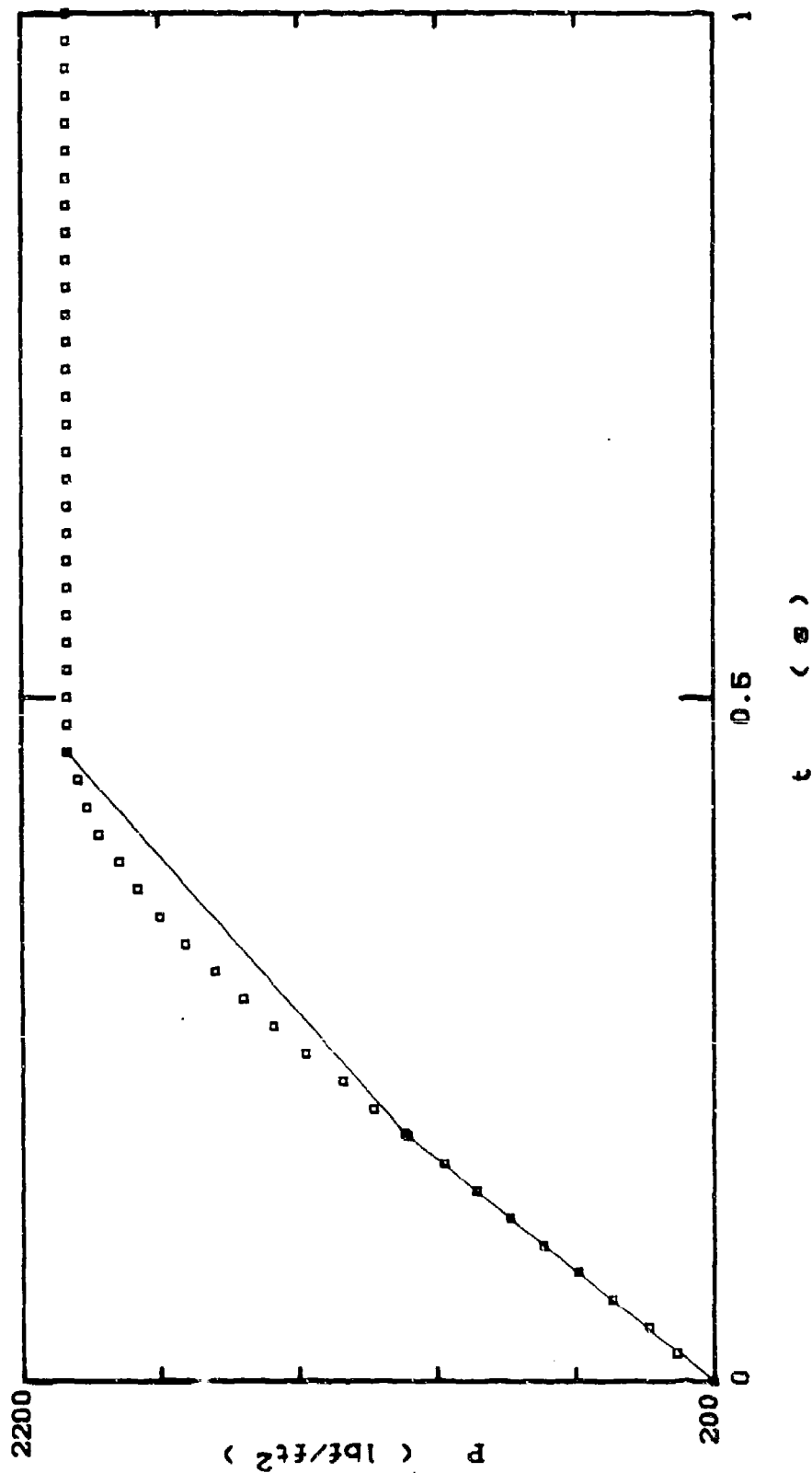
Figure 6-4   Straight Line Approximation to Pressure Curve
Used in Finding t_{uc} and t_p

The pressures are measured in lbf/ft^2, and the times are in seconds. These two equations are only valid for the nozzle and tank that was used in this study. Since the time to fill a tank ought to be proportional to the volume of the tank, Eq. [6-1] was multiplied by the ratio of new tank volume, V, to the tank volume used in this study. Also, a nozzle with a large throat area will fill a tank faster than one with a small throat area. Thus, Eq. [6-1] was divided by the ratio of new throat area, A_{th}, to the area of the throat that was used. These equations are

$$t_{uc} = 0.003362 \; (V/A_{th})(0.52828P_0 - P_1) \; / \; 4952.25$$

[6-2]

$$t_p = t_{uc} + 0.001585 \; (VP_0/A_{th}) \; / \; 3481.71$$

The tank volume is measured in ft^3 and the throat area in ft^2. Equation [6-2] can now be used to estimate the time it takes for a given nozzle to unchoke as well as the time required for the gas in the tank to reach equilibrium pressure.

From the data in Figure 5-14, the the heat transferred by t_p is approximately 50% of Q_{tot}. Also, from Figure 6-2, $\dot{Q}(t)$ can be accurately approximated by a second order polynomial between $t=0$ and $t=t_p$.

$$\dot{Q}(t) = \dot{Q}_{max} \; [at^2 + bt + c] \qquad [6-3]$$

The following equation can then be used to find Q_{max}.

$$0.5 \ Q_{tot} = \dot{Q}_{max} \int [at^2 + bt + c] \ dt \qquad [6-4]$$

The three conditions needed to find the coefficients are

$$\dot{Q}_{max} = \dot{Q}(t_{uc})$$

$$\dot{Q}(0) = 0$$

$$\dot{Q}(t_p) = 0.18 \ \dot{Q}_{max}$$

Therefore,

$$\dot{Q}(t) = \dot{Q}_{max} t \ [8.875 - 18.444 \ t] \qquad [6-5]$$

After substituting into Eq. [6-4] and integrating,

$$\dot{Q}_{max} = 0.5 \ Q_{tot} \ / \ [t_p^2 (4.4375 - 6.148 t_p)] \qquad [6-6]$$

Thus, by knowing only the volume of a tank, the area of the nozzle throat, the ambient pressure, and the initial pressure within the tank, the total heat transferred to the tank walls can be calculated. Also, the times to unchoking and pressure equalization can be estimated as can the peak heat flux and the shape of the $\dot{Q}(t)$ curve. The remainder of the $\dot{Q}(t)$ curve can also be estimated after t_p by assuming another second order polynomial. This part of the curve represents long times with small heating rates. Because of this, the first part of the curve is most important and was all that was found. However, the total time for charging to

be completed can be estimated by

$$t_f = 22 \, t_p \qquad\qquad [6-6]$$

This equation was found by taking the measured ratio of the total time for charging, 10 seconds, to the time at which the tank pressure equaled P_o, 0.46 second.

VII. Summary

This study was a new look into the old problem of charging a vessel with an ideal gas. The actual transient process was observed and calculated. A major suprise was the uniformity of heat flux along the walls of the tank. There were no significantly hot or cold spots at any point on the tank wall. Another suprise was the strange behavior of the convection coefficient with respect to (ρu). As a result, it was difficult to make any conclusive statements as to the actual flow dynamics. It was also difficult to formulate a method of using $h(t)$ for the prediction of heat transfer rates in other tanks. However, a method of estimating peak heating rates as well as the general shape of the $\dot{Q}(t)$ data was found.

VIII. Recommendations

Further study of the charging process is definitely warranted. This study, being the first of it's kind, has only scratched the surface of the complexities involved in the flow dynamics and heat transfer during the charging of an evacuated tank. Further experimentation should involve the recording of heat transfer data throughout the entire process. Also, testing with different nozzle sizes and various pressure conditions should be carried out to verify or disprove the estimation techniques developed here. It would also be of interest to vary the length to diameter ratio of the tank in order to determine effects resulting from geometry. All these would aid in developing a means of accurately predicting heat flux during the charging process.

Appendix A

Model Numbers of Equipment Used

Endevco 0-100 psia Pressure Transducer .... Model # 8530A-100

TSI Miniature Flush Mount

Sensor Elements .... 1268 Platinum Hot Flim

Probes used: 1, 2A, 3, 4, 8

Datalab dl1200 Waveform Recorder .... Serial # 119

Appendix B

Table of Heats Measured by Individual
Thin-Film Gages

* LOCATION ON THE TANK WALL	TRIAL NUMBER FOR GAGE	HEAT LOSS PER AREA BTU/FT^2	WALL AREA REPRESENTED IN^2	TOTAL HEAT LOST BTU
1	**	0.2655275	28.274	0.0521356
2	E2	0.4253386	47.124	0.1391921
3	E3	0.4508400	56.941	0.1782728
4	D3	0.3764253	78.540	0.2053086
5	D4	0.2168532	94.248	0.1419304
6	D5	0.3276899	94.248	0.2144730
7	C3	0.4223368	94.248	0.2764194
8	C4	0.2916098	94.248	0.1908586
9	E4	0.3129244	94.248	0.2048090
10	B3	0.4977912	94.248	0.3258043
11	B4	0.3131344	94.248	0.2049465
12	B5	0.4033936	94.248	0.2640211
13	F3	0.4254639	94.248	0.2784661
14	F4	0.2767622	78.540	0.1509507
15	F5	0.3774505	62.832	0.1646942
16	F2	0.3742415	34.361	0.0893008
17	B2	0.3950619	28.274	0.0775693
18	C2	0.3618079	14.137	0.0355200
19	D2	0.3845312	1.767	0.0047185

TOTALS 1279.022   3.1993912

*   For locations, see Fig. 6-1, page 50.

**	B1	0.2407778	
	C1	0.2777149	
	D1	0.2814635	Gage left in same spot on
	E1	0.2444963	tank for 5 runs to verify
	F1	0.2831850	experiment repeatability.
	AVERAGE	0.2655275	

Bibliography

1. Jones, J. B. and Hawkins, G. A. <u>Engineering Thermodynamics</u>. New York: John Wiley and Sons, Inc., 1986.

2. Wark, Kenneth. <u>Thermodynamics</u>. New York: McGraw-Hill Book Co., 1977.

3. Frye, J. W., Jr. <u>Thin Film Heat Transfer Gages</u>. MS thesis, GAM/ME/66A-3. School of Engineering, Air Force Institute of Technology (AU), Wright-Patterson AFB OH, 1966.

4. Duffy, Dean G. <u>Solutions of Partial Differential Equations</u>. Blue Ridge Summit, PA: Tab Professional and Reference Books, 1986.

5. Cook, W. J. and Felderman, E. J. "Reduction of Data from Thin-film Heat Transfer Gages: A Concise Numerical Technique," <u>AIAA Journal</u>, $\underline{4}$ (3): 561-562 (March 1966).

6. Shapiro, Ascher H. <u>The Dynamics and Thermodynamics of Compressible Fluid Flow</u>. New York: John Wiley and Sons, Inc., 1953.

Vita

Dennis E. Lileikis was born August 13, 1963 in Chicago Heights, Illinois. He graduated from Marian Catholic High School, Chicago Heights, Illinois in 1981 and was the valedictorian. He then attended the College of Engineering at the University of Illinois under an AFROTC scholarship. He graduated with honors in May 1985 and received a B.S. in Aeronautical and Astronauical Engineering. The same month, he was commissioned into the Air Force and was assigned to the Air Force Institute of Technology.

Permanent address: 22543 Jeffery Avenue

Sauk Village, IL 60411

HD-A172 816

REPORT DOCUMENTATION PAGE

Form Approved
OMB No. 0704-0188

1a. REPORT SECURITY CLASSIFICATION	1b. RESTRICTIVE MARKINGS
UNCLASSIFIED	

2a. SECURITY CLASSIFICATION AUTHORITY	3. DISTRIBUTION/AVAILABILITY OF REPORT
	Approved for public release;
2b. DECLASSIFICATION/DOWNGRADING SCHEDULE	distribution unlimited.

4. PERFORMING ORGANIZATION REPORT NUMBER(S)	5. MONITORING ORGANIZATION REPORT NUMBER(S)
AFIT/GA/AA/86D-9	

6a. NAME OF PERFORMING ORGANIZATION	6b. OFFICE SYMBOL (If applicable)	7a. NAME OF MONITORING ORGANIZATION
School of Engineering	AFIT/ENY	

6c. ADDRESS (City, State, and ZIP Code)	7b. ADDRESS (City, State, and ZIP Code)
Air Force Institute of Technology Wright-Patterson AFB, Ohio 45433	

8a. NAME OF FUNDING/SPONSORING ORGANIZATION	8b. OFFICE SYMBOL (if applicable)	9. PROCUREMENT INSTRUMENT IDENTIFICATION NUMBER

8c. ADDRESS (City, State, and ZIP Code)	10. SOURCE OF FUNDING NUMBERS			
	PROGRAM ELEMENT NO.	PROJECT NO.	TASK NO	WORK UNIT ACCESSION NO.

11. TITLE (Include Security Classification)
UNSTEADY HEAT TRANSFER RESULTING FROM THE RAPID CHARGING OF AN EVACUATED TANK WITH CONDUCTING WALLS   (UNCLASSIFIED)

12. PERSONAL AUTHOR(S)
Lileikis, Dennis Earl

13a. TYPE OF REPORT	13b. TIME COVERED	14. DATE OF REPORT (Year, Month, Day)	15. PAGE COUNT
MS Thesis	FROM _____ TO _____	1986 December	73

16. SUPPLEMENTARY NOTATION

Approved for public release. IAW AFR 190-1.
LYNN E. WOLAVER   13 MAR 87
Dean for Research and Professional Development
Wright-Patterson AFB OH 45433

17.	COSATI CODES		18. SUBJECT TERMS (Continue on reverse if necessary and identify by block number)
FIELD	GROUP	SUB-GROUP	Heat Transfer, Charging of Vessels, Convection,
20	13		Unsteady Heat Transfer

19. ABSTRACT (Continue on reverse if necessary and identify by block number)

This study went beyond equilibrium analyses to acquire a fundamental understanding of the transient phenomenon involved in the charging of a vessel. By way of experimentation, transient pressure and heat flux measurements were made on an evacuated cylindrical tank as it was charged by sudden exposure to the atmosphere. An average convection coefficient and a driving temperature potential were found. A method was developed for predicting heating rates in other tanks. The distribution of the heat flux on the tank walls was discovered. From all the measured data, information about the transient flow dynamics was gleaned. This information includes rates of kinetic, internal, and thermal energy generation and dissipation as well as rates of entropy creation in the gas.

20. DISTRIBUTION/AVAILABILITY OF ABSTRACT	21. ABSTRACT SECURITY CLASSIFICATION
☒ UNCLASSIFIED/UNLIMITED ☐ SAME AS RPT. ☐ DTIC USERS	UNCLASSIFIED
22a. NAME OF RESPONSIBLE INDIVIDUAL	22b. TELEPHONE (Include Area Code)	22c. OFFICE SYMBOL
James Hitchcock, Professor, AFIT	513-255-3517	AFIT/ENY

DD Form 1473, JUN 86   Previous editions are obsolete.   SECURITY CLASSIFICATION OF THIS PAGE
UNCLASSIFIED